A MATHEMATICAL MODEL OF DRUG DELIVERY BY MODIFYING THE TUMOR MICROENVIRONMENT: MMP ACTIVATION

by

Duygu Kaba

B.S., Mathematics, Boğaziçi University, 2010

Submitted to the Institute for Graduate Studies in
Science and Engineering in partial fulfillment of
the requirements for the degree of
Master of Science

Graduate Program in Graduate Program in Mathematics

Boğaziçi University

2013

A MATHEMATICAL MODEL OF DRUG DELIVERY BY MODIFYING THE TUMOR MICROENVIRONMENT: MMP ACTIVATION

APPROVED BY:

Assoc. Prof. Burak Gürel .....
(Thesis Supervisor)

Assoc. Prof. Mehmet Burçin Ünlü .....
(Thesis Co-supervisor)

Assoc. Prof. Burak Acar .....

Assist. Prof. Fatih Ecevit .....

Assoc. Prof. Atilla Yılmaz .....

DATE OF APPROVAL: 13.06.2013

ACKNOWLEDGEMENTS

I would like to thank deeply to my thesis supervisor, Assoc. Prof. Burçin Ünlü. His sincerity, guidance and tolerance together with his vivid and bright smile were sufficient to push forward me with a great motivation. I owe my profound gratitude to Assoc. Prof. Burak Gürel for his valuable mentoring and to Prof. Alp Eden since during my undergraduate and graduate studies, his enthusiasm and guidance has become my driving force. It was an honor and pleasure to be a student of them.

I would like to thank to Assist. Prof. Fatih Ecevit, Assoc. Prof. Atilla Yılmaz and Assoc. Prof. Burak Acar for participating in my thesis committee with their valuable comments. My special thank is to Hakan Erkol for his detailed reading of my drafts and his corrections with patience.

I gratefully acknowledge TÜBİTAK for providing me with scholarship.

I wish to thank all my officemates in the Department of Mathematics and all members of our Research Group for their contribution to a friendly atmosphere. Şirin Yonucu and Deniz Öztürk deserve special thanks for sharing their knowledge about modeling. Moreover, *the fabulous five* will never be forgettable! I am thankful to Murat Güner for his great collaboration to embrace all of us; to Güneş Şenel for her true friendship and endless patience; to Güher Çamlıyurt for her support and desire to study and travel with us. They were the passenger of the same way who shared with me the same stress through our application process and own thesis studies.

I dedicate my thesis to my parents and Emre Demirkaya due to their endless support and confidence throughout my education. Finally, I never hesitate to say that with his endless love and affection, Emre is far beyond to be my life source, best friend, joyful colleague and wise advisor.

ABSTRACT

A MATHEMATICAL MODEL OF DRUG DELIVERY BY MODIFYING THE TUMOR MICROENVIRONMENT: MMP ACTIVATION

Cancer modeling has become one of the challenging frontiers of applied mathematics mostly for two decades. Drug delivery to solid tumors also attracts both theorists and experimentalists due to its significance in cancer therapy. Recent studies have revealed that drug responses of tumor cells are determined both by intrinsic characteristics and by regulation of tumor microenvironment. The irregularity tumor blood vessel structure results in disorganized blood flow within the tumor and increased leakage which causes increased interstitial fluid pressure (IFP). This IFP forms a barrier for drug transport and it could be seen as an apparent obstacle to the delivery of therapeutic molecules. The basis of this thesis is the effects of the delivery of matrix metalloproteinases (MMPs) to the tumor tissue, which in turn, increased hydraulic conductivity, improved interstitial transport and enhanced distribution of nanotherapeutics. In the light of Mok *et al.*'s researches, a mathematical model which associates the effect of MMPs to convective transport and to drug distribution in tumors is constructed. Governing equations in the model with suitable boundary conditions involve the principles for transvascular and interstitial drug transport and conservation laws. Finally, these equations are discretized with finite element method (FEM) and the simulation results are discussed comparing to the literature.

ÖZET

TÜMÖR MİKROÇEVRESİNİN DEĞİŞTİRİLMESİ YOLUYLA İLAÇ İLETİMİNİN MATEMATİKSEL MODELLEMESİ: MMP AKTİVASYONU

Kanser modellemesi, özellikle son yirmi sene içinde, uygulamalı matematiğin zorlu bir keşif sahası haline gelmiştir. Ayrıca katı (solid) tümörlere ilaç iletimi hem teorisyenleri hem de uygulamacıları tedavideki önemi sebebiyle cezbetmektedir. Son çalışmalar, tümör hücrelerinin ilaca verdikleri tepkinin hem iç özellikleriyle hem de tümör mikroçevresinin tanzimiyle belirlendiğini ortaya koymuştur. Tümör kan damar yapılanmasındaki düzensizlikler tümör içinde dağınık bir kan akışına ve interstisyel sıvı basıncının (İSB) artışına sebebiyet veren sızıntıların artışına neden olur. İSB ilaç iletimi için bir bariyer oluşturur ve iyileştirici moleküllerin iletimine bariz bir engel olarak görülebilir. Bu tezin temeli matriks metalloproteinazların (MMP) tümör dokusuna etkileridir; bu etkiler sırasıyla, artan hidrolik geçirgenlik, gelişen interstisyel taşınımı ve nano-iyileştiricilerin dağılımının çoğalmasıdır. Mok ve çalışma arkadaşlarının araştırmalarının ışığı altında, MMPlerin konvektif taşınıma ve ilaç dağılımına etkisini ilişkilendiren bir matematiksel model inşa edilmiştir. Modeldeki hakim denklemler uygun sınır koşullarıyla birlikte, transvasküler ve interstisyel ilaç taşınım ilkeleri ve korunum yasalarını içerir. Son olarak, bu denklemler sonlu eleman metoduyla (SEM) ayrıklaştırılmış ve simülasyon sonuçları literatürle karşılaştırılarak tartışılmıştır.

TABLE OF CONTENTS

LIST OF FIGURES

LIST OF TABLES

LIST OF SYMBOLS

c	Tissue drug concentration
c_0	Maximum plasma concentration of drug after injection
c_p	Plasma drug concentration
$\mathbb{C}$	Complex numbers
$C^1[a,b]$	Space of continuously differentiable functions on an interval $[a,b]$
D_c	Diffusion coefficient of drug in the tissue
D_E	Effective diffusion coefficient of MMPs in tumors
D_M	Diffusion rate of MMP molecules in the tissue
$H^1[a,b]$	Sobolev space on an interval $[a,b]$
k_E	Retardation coefficient for transvascular convection
K	Hydraulic conductivity of tissue
K_0	Hydraulic conductivity of tissue at zero deformation
$L^2[a,b]$	Space of square integrable functions on an interval $[a,b]$
L_p	Vessel wall hydraulic conductivity
M	MMP concentrations in the tissue
M_p	MMP concentrations in the plasma
n	Average tumor cell density
$\mathbf{n}$	Unit outward normal vector
$\mathbf{N}$	Natural numbers
P	Interstitial fluid pressure
P_0	Vascular fluid pressure
q_F	Interstitial fluid flux
$\mathbb{R}^n$	n-dimensional Euclidean space
R_0	Tumor radius
$Re(z)$	Real part of a complex number z
$t_{1/2}$	Half life of drug concentration
$\mathbf{v}$	Vector
$\mathbf{v}_F$	Velocity of the interstitial fluid

$\overline{z}$	Conjugate of z in complex numbers
Γ_{Fb}	Supply of fluid from blood vessels to the interstitial space
Γ_{Fl}	Drainage of fluid from the interstitial space into lymph vessels
λ_d	Transvascular diffusion coefficient of drug
λ_{Fb}	Hydraulic conductivity of blood vessel networks
λ_{Fl}	Hydraulic conductivity of lymph vessel networks
λ_{Md}	Transvascular diffusion rates of MMP molecules
λ_{Mn}	Production rate of MMP molecules by tumor cells
λ_{Mr}	Decay rate of MMP molecules by tumor cells
λ_r	Decay rate of drug
π_c	Capillary osmotic pressure
π_i	Interstitial osmotic pressure
σ	Osmotic reflection coefficient
ϕ_F	Volume fraction of interstitial fluid
ϕ_h	Heterogeneity of drug distribution
Φ_e	Total tumor exposure
Ω_N	Normal tissue domain
Ω_T	Tumor domain
$:=$	Definition
$\langle \, . \, \rangle_X$	Inner product of a Hilbert Space X
$\| \, . \, \|_X$	Norm of a normed vector space X
∇f	Gradient of f
$\nabla \cdot \mathbf{v}$	Divergence of $\mathbf{v}$
$\frac{\partial f}{\partial x_i}$	Partial derivative of $f(x_1, x_2, \ldots, x_n)$ with respect to x_i

LIST OF ACRONYMS/ABBREVIATIONS

BM	Basement membrane
DC101	Anti-VEGF2 antibody
DNA	Deoxyribonucleic acid
ECM	Extracellular matrix
FEM	Finite element method
GAG	Glycosaminoglycan
GM6001	Broad spectrum MMP inhibitor
HGF	Hepatocyte growth factor
HSV	Herpes simplex virus
IF	Interstitial fluid
IFF	Interstitial fluid flux
IFP	Interstitial fluid pressure
MMP	Matrix metalloproteinase
MRI	Magnetic resonance imaging
MMPi	Matrix metalloproteinase inhibitor
MT-MMP	Membrane type matrix metalloproteinase
PDE	Partial differential equations
PET	Positron emission tomography
pO_2	Oxygen tension
TAF	Tumor angiogenic factor
TSG	Tumor suppressor genes
VEGF	Vascular endothelial growth factor

1. INTRODUCTION

"Mathematics is Biology's next microscope, only better; Biology is Mathematics' next Physics, only better."-J. E. Cohen

Applied mathematicians need to pursuit new ideas and concepts, which may form new classes of equations to be handled with by advanced analytic and computational methods. The development in the branches of science and engineering has become possible by the advancement of mathematics. Especially, the theories and laws in physics have gone hand in hand with the mathematical facts and theories. The history of mathematical biology which is considerably new comparing to the relation between mathematics and physics, is about 30-40 years. Accordingly, *cancer* is one of the highly demanding topic worked on by mathematicians, physicians, biologists and medical scientists. If this cross-pollination have not been occurred, then the mutual understanding and appreciation on the part of experimental and theoretical scientists would have lacked. During the last ten years, a lucid advancement of mathematical modeling and methods have been experienced. In the same period, mathematics and medicine have been interacted quantitatively and qualitatively improved going from an intellectual aim to a significant interaction and collaboration. One of the reason of this interdisciplinary interest stems from the remarkably high death rate in the world especially in western countries. By 2030, 21.4 million new cancer cases and 13.2 million cancer deaths are expected all over the world (http://www.cancer.org/research/cancerfactsstatistics/global). Although the positive therapy has been successful at least for some pathologies, a visible effort of human and economical resources have been devoted to cancer research [8]. Experiments in the laboratories that control their hypotheses could be expensive, difficult with current technological devices or require long hours. Moreover, the results might vary under mice and human bodies. One of the difficulties is also the uniqueness of tumor growth to each member. Apparently, a result obtained from one patient might not give satisfactory effects to other patients. Neither time nor budget can be sufficient to deal with and solve each patient's specific disease. The phenomena could be explained by

mathematical system of equations by the aid of some physical law and principles. This helped to create a new subcategory under the applied mathematics: "Mathematical Biology". Particularly, "Modeling" has become one of the trend subjects to work on. As Bryne describes, mathematical modeling has a buffer role between the theory and the applications. If the hypothesis gives contradictory results within the model, then the hypothesis might be revised after testing the validity of model by a rich source of parameters, and this process occurs without the costs of experiments. Likewise, a mathematical model could make the experimental design stronger and help it to be selective about which measurements and data are required. There are variegated number of models explaining tumor growth, tumor microenvironment and drug delivery to the tumors. Even though mathematical modeling seems as a good alternative for experiments, biological systems do not work similar with the physical or chemical systems which have principles from statistical mechanisms or hydrodynamics. Statistical mechanics typically behaves systems as consisting many copies of few interacting components while cells owe from millions to a few copies of thousands of different components, each with very specific interactions [9]. Even though these existing mathematical models may not explain the entire biological phenomena, they are the initial steps to combine reasoning and intuition [10]. Furthermore, the relation between biology and mathematics might be seen as a loop having a positive feedback. Mathematics has an impact of easing the experiments and their results while biology gives a chance to the applied mathematicians to become motivated by interesting and challenging mathematical problems that yield new mathematical methods and theories. As an example the mathematical theory of free boundary problems has been developed by the construction of new mathematical models inspired from the changes in biology. The tumor models have described a new class of free boundary problems related to symmetry-breaking bifurcations of a spherical tumor and its stability [11].

Our aim in this thesis is integrating the tumor microenvironment and drug delivery with the light of some articles and theses. We try to answer "How can drugs enhance the interstitial transport and improve the treatment of solid tumors with the aid of some specific matrix metalloproteinases (MMPs)?" during the thesis. Concerning this question, we start with categorizing the models and explaining their advantages

and drawbacks. In Chapter 2, we give a necessary biological background to help to understand the insight of the models. In order to do this, some biological terms like MMP, ECM, IFP are investigated. MMPs notably pose a crucial situation in our model and we reveal their positive and negative effects comparing to their kinds.

In Chapter 3, we start to construct our model regarding three sections: We need to simplify this complex phenomena so some necessary assumptions are explained. After that, the derivation of mathematical equations (mostly PDEs) plays an important role and we consider the boundaries of the problem. The therapy and then its application to our model are discussed.

Chapter 4 concerns the simulation of our model so we attempt to give a motivation for Finite Element method (FEM). Its mathematical theory is explained with Galerkin approximations and it is applied to our model.

Chapter 5 deals with the results of our model, we discuss through the graphics and plots. Some parameters are known from the literature while some of them are estimated. Integrating all the necessary information, we try to interpret the results.

In Chapter 6 which is the conclusion chapter, we discuss our model and future work.

1.1. Significance of Mathematical Modeling

Why does mathematical modeling become so popular and a part of interdisciplinary study? Experiments is an inevitable part of the biological sciences, which compel scientists to study in laboratories for hours, even days. Simulations and models do not only diminish the amount of time and experiments, they also make it possible to analyze errors before clinical trials. Experiments reinforced with the mathematical modeling approach can be used to generate and test hypotheses while the results of experiments help to refine the modeling. The mathematicians eventually develop a deeper understanding of how the nonlinear processes and biology interact with this

positive feedback between theory and experiments. On the contrary, the scientists aim to use mathematical models in the clinical trials to help design therapeutic strategies. Mathematical models serve to combine different results and give rise to both simple and complex explanations of cancer disease process. Their tools provide to enhance hypotheses about entire lifespan of tumor from its appearance to treatment. The amount of experiments necessary for drug and therapy development can be reduced with the aid of modeling and simulations. The mathematical modeling of cancer provides simulation of a variety of tumor growth patterns which is not always observed in the laboratories.

Helen Byrne [1] compares physics to biology with the following illustration: "The similarity to the physical models that include the expansion of metals with heat and freezing of liquids gave a deep motivation to the mathematicians to colloborate with biologists and to create models from these biological phenomena. In this case, the size of tumor changes over time as in the metal or solid case, likewise the tumor's growth rate is regulated by the transport of oxygen or glucose as in the temperature change for the metal and liquid."

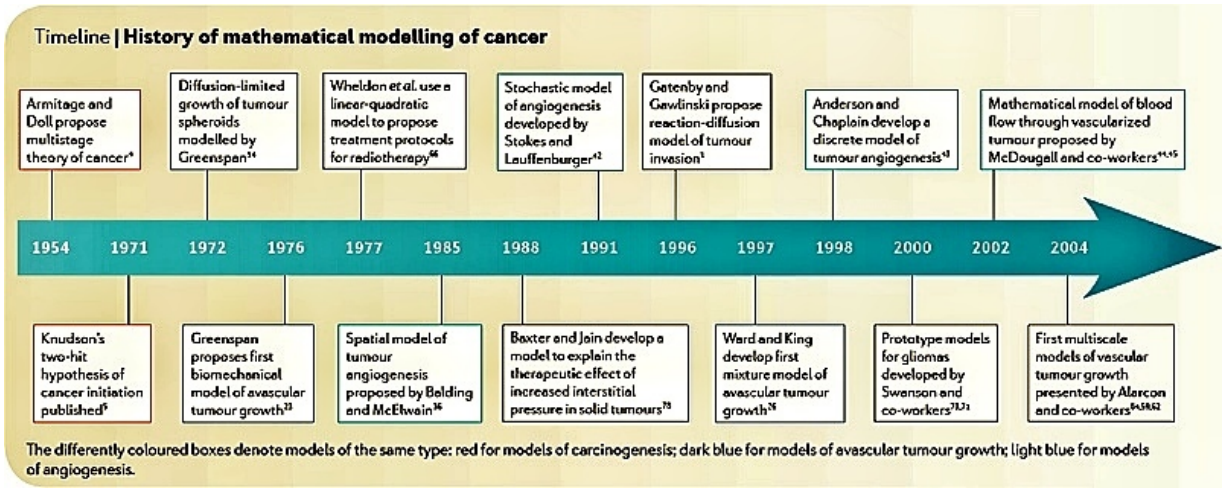

Figure 1.1. Timeline for Mathematical Modelling [1].

Applied mathematicians focusing on mathematical modeling should answer the following questions:

- How to select an appropriate mathematical framework among existing ones?
- How to establish links between models at the selected scale and models at lower and higher scales?

1.1.1. Multiscale Aspects of Cancer Modeling

The biological system in cancer modeling is de facto a multiscale mathematical approach. Scaling which ranges from genes to tissues requires different functions is defined at different scales.

We can classify natural scales in three distinct scales:

- Cellular scale: Refers to main activities of the cells. For instance, activation, proliferation and interactions between tumor cells and the immune system might be considered.
- Sub-cellular scale: Refers to activities that take place within the cell or at the cell membrane. It focuses on
  (i) The aberrant activation of signal transduction pathways that control cell growth and survival,
  (ii) Response of the cellular activity to the signals received,
  (iii) Absorption of vital nutrients. (Gatenby and Maini 2003 [10])
- Macroscopic scale (which we use in our model): Refers to those phenomena which are typical of continuum systems such as cell migration, convection, diffusion of chemical factors, detached cells, metastasis and phase transitions. In these models, the cells might be considered as a single continuum due to their large numbers. So rather than observing individual cell activities, conservation laws for densities are valid that change with time and space coordinates. These models deal with length scales on the order of mm cm and time scales on the order of day year. One should be aware of the fact that in subcellular and cellular scale models, it is relatively more difficult to obtain parameters via experiments comparing to the macroscopic ones.
- Multiscale: From a biological or physiological point of view, a model is considered

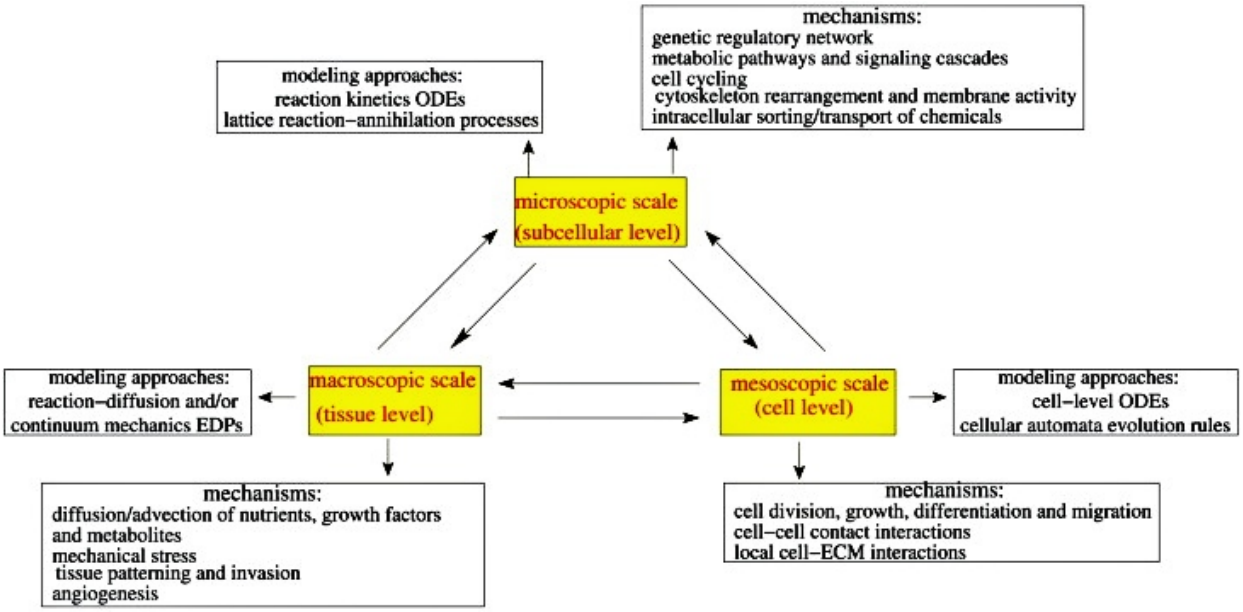

Figure 1.2. Classification of Natural Scales [2].

to be "multiscale" if it spans two or more different space coordinates scales or contains processes occurring at two or more time scales. However, quantifying parameters at different scales makes the model more complex even though it seems more realistic [12].

Keeping in view our motivation, drug delivery is a tranport problem and as explained by Netti and Jain (2003) [13], "There are two interlaced aspects one has to be aware of in modeling this process: the influence of the size of the drug and the mechanisms driving the transport and the diffusion of the drug."

1.2. Different Model Types

The number of model types and their differentiation result from their specialization and motivation. A general method is to take the cell population into account. Thanks to [14] and [15], we can categorize these models under some headings:

- (Continuous Model) If the number of cells are greater than a million, continuum models are preferred. The densities of various types of cells are mainly considered. For instance, the properties of a cell with its growing, viable and necrotic part

are averaged over a mass of cells of a given type. PDEs generally describe this type of models.

- (Cellular Automata Model) Each cell is represented as a separate entity and its properties occupy one site of a regular square lattice. A series of rules depend on each separate cells so it is easy to translate biological processes with this method. This model is also useful in informing medical treatment decisions. However, only 1 mm tumor spheroid has over 500.000 cells and the computational cost and the number of cells are positively related. Since there are many equations in this modeling framework, models behave in byzantine fashion and the analysis becomes based on simulation. Monte-Carlo simulations are used.
- (Particle-Based Model) This is an off-lattice center-based particle model and cells are defined as individual overlapping points. The technique is based on potential energy.
- (Cellular Potts Model) In this model, every cell is composed of several lattice sides which allows the representation of cell shape and deformations. They depend on energy minimization.
- (IBCell Model) In this model, every cell can have variable shapes and it is modeled as an elastic body immersed in a viscous incompressible fluid.

Cellular automata and agent (particle) based modeling are generally preferred for studying carcinogenesis, genetic instability, cell motility and interactions of individual cells with each other and the microenvironment.

Continuum models have a common denominator, since they explain how cell concentrations are exposed to change and contrary to the discrete models, they do not distinguish each cells separately. The stochastic effects are generally ignored. So a choice of a model depends tightly on the number of cells: If you are studying on growth kinetics of tumor spheroids of large number of cells, the continuum models suit better. However, for a small cluster of cells (metastases), discrete models like cellular automata might be a better choice to work on. In discrete models, the cells are seen as interacting cells with each other and each individual cell has its own parameter values and distinct behaviours. Despite its complexity, some of the mathematicians

have developed a hybrid model that includes equations of both continuum and discrete models. When a region has a high tumor density, they use a continuum model here, and the regions that have only few numbers of tumor cells require discrete model.

Beyond the types and their application areas, mathematical modeling could pose an influential role for the integration of images obtained by using different modalities. For instance, Swanson and her team reported a strong correlation between the invasiveness and degree of hypoxia of gliomas, the estimate of invasiveness comes from magnetic resonance imaging (MRI) data while 18 F-fluoromisonidazole-positron emission tomography (PET) images help to estimate of hypoxia. Hence, a new mathematical model could be constructed that links hypoxia and invasion which combine the estimations from the MRI data and PET images. So the collection of images for diagnosis which may be under different conditions is a demanding topic where mathematics has a pivot role.

In this thesis, we attempt to shed light on innovative findings of Wilson Mok's PhD thesis [16] comparing with the literature. His hypothesis which is the delivery of a matrix- modulating enzyme to the tumor interstitium can improve the convective transport and the efficacy of a macromolecular cancer therapeutics. They generate novel oncolytic HSV (Herpes simplex virus) vectors which express MMP1 or MMP8. These proteases have multiple matrix substrates and it is observed that they are able to make a significant reduction in the tumor of sulfated glycosaminoglycans (GAGs) known as negatively correlated by the convective transport.

The interesting part is: In MMP-1 and MMP-8 expressing tumors, the hydraulic conductivity was more than *two-fold greater* than the mock transfected. Furthermore, it is experimented that HSV particles were present only in the periphery of the tumor, while for MMP1 and MMP8 expressing tumors, HSV particles were located in both the periphery and the center of the tumor. So, it is necessary to glance the tumor microenvironment, the flow of interstitial fluid and matrix metalloproteinases.

2. BIOLOGICAL BACKGROUND

In this chapter, we try to understand the biological side of model. We mainly refer to the studies of Macklin *et al.* [3], Jain *et al.* [4] and Rejniak *et al.* [14].

2.1. Tumor Growth

The structure of the stroma and epithelial cells gives a clue for tumors. The epithelium is composed of sheets of tightly bound epithelial cells that cover organ surfaces and perform specialized functions. This epithelium is supported by the stroma which is a loose connective tissue. The main component of the stroma is the extracellular matrix (ECM) and it is described by bundles of fibers (e.g, collagen, elastin, fibronectin) embedded in a mixture of water and glycoproteins. The ECM is secreted and maintained by stromal cells which are specialized mesenchymal cells that can freely move within the stroma as they maintain the tissue. Fibroblasts are the primary stromal cells in loose connective tissue (epithelial stroma). The stroma is embraced by blood vessels, nerves, and lymphatic vessels. A thin, semi-permeable basement membrane (BM, a specialized type of ECM) separates the epithelium from the stroma.

There are some control mechanisms on growth and proliferation process. On one hand, epithelial cell cycle progression and proliferation are partly controlled by cell-cell adhesion. When an epithelial cell is in contact with many neighbors, its cell cycle and proliferation are restrained. Correspondingly, the presence of contact among them helps to prevent overproliferation. The cell populations are also controlled by contact with the extracellular matrix and basement membrane.

On the other hand, the balance between growth and inhibitory signals is necessary for a healthy tissue. Two types of genes are found to be particularly relevant to regulating cell proliferation. Oncogenes create growth signals and promote cell cycle progression while tumor suppressor genes (TSGs) respond to inhibitory signals, retard or cease the cell cycle. TSGs are also able to ensure proper DNA repair and under

certain circumstances, apoptosis might occur. The breakpoint of this balance; in other words, cancer initiation termed as "carcinogenesis" starts with the malfunction of one or more of those types of genes. If the cell survives and the mutation escapes from DNA repair mechanisms, then the cell may over time acquire further mutation that enable it to neglect growth-inhibitory signals from its neighbors, its internal controls and check points. As a result, these mutated cells form a colony of hyperproliferative aberrant cells.

Differentiated cells can be only divided a limited number of times before reaching senescence the point at which they permanently arrest in Gap 0 (G_0) or apoptose. So differentiated cells alone cannot drive unlimited tumor growth without additional mutations to overcome senescence. However, contrary to the common belief, recent studies propose that cancer may arise from mutated somatic stem cells rather than differentiated cells. Tumor is thereby a mixed cell population whose overgrowth is driven by a small subpopulation of cancer stem cells rather than by differentiated cells that have overcome senescence.

2.1.1. Avascular Solid Tumor Growth

In early stages, the tumor has no vascular system on its own. So this requirement is fulfilled by host vasculature in the nearby stroma for crucial oxygen, nutrients and growth factors where they are termed as substrates.

Substrates diffuse from the surrounding vascularized tissue, enter the tumor, and are uptaken by proliferating tumor cells. The motion from host vasculature to the internal sinks results in substrate gradients. Especially for oxygen, the diffusion is order of 100-200 μm into tissue and lacking from this amount causes hypoxia (oxygen insufficiency) which ends up by necrosis. The evaluation of tumor growth can be summarized as the followings:

(i) Before a necrotic core occurs, proliferation throughout the tumor causes a net outward flux that expands the tumor. At the same time, the proliferating tumor

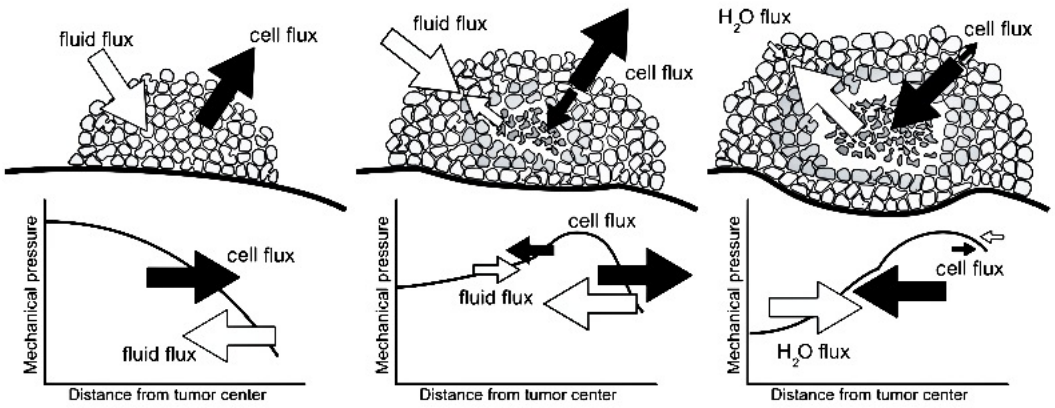

Figure 2.1. Cell and Fluix Flux in Early (Left), Later (Middle), and Long Time (Right) Tumor Growth [3].

cells absorb fluid from the interstitium to fuel their growth and eventual division yield net fluid flux into the tumor.

(ii) When necrotic core forms cell lysis, it reduces the tumor cell volume and releases fluid that leaves the necrotic core and enters the proliferative rim interstitium. This reduction in mechanical pressure in the necrotic core redirects some of the viable rim cell flux towards the tumor interior. Meanwhile, as the tumor grows, the volume of its necrotic core increases which accentuates its cell volume sink effect.

(iii) If tumor growth is large enough, cell flux resulting from proliferation balances with the fluid flux stemming from necrosis and this leads to zero outward cell flux. At the end, steady-state tumor spheroid is observed.

2.1.2. Vascular Growth and Metastasis

The tumor mechanically displaces and compresses the surrounding tissue. After then, it degrades and remodels the extracellular matrix (ECM) both biomechanically and biochemically by the secretion of enzymes like MMPs that degrade the ECM. The degraded ECM, in turn, can release ECM-associated growth factors that trigger fur-

ther tumor growth. The combination of proliferation induced pressure and proteolytic degradation of the surrounding tissue results in tissue invasion which can be expressed as the invasion of sheets or "fingers" of tumor cells into the surrounding tissue along the paths which require least mechanical resistance.

These stages are responses to hypoxia and hypoxic microenvironment which leads to angiogenesis. Angiogenesis is the critical process in which the tumor induces endothelial cells to form a new vasculature that directly supplies the tumor with the nutrients enabling further expansion. This occurs with the secretion of tumor angiogenic factors (TAFs) of hypoxic cells such as vascular endothelial growth factor (VEGF). These TAFs diffuse outward from the hypoxic regions of the tumor and eventually reach nearby blood vessels. As a result, the spread of tumor cells to distant locations which results in metastasis might be possible and metastasis is the worst process in cancer evaluation.

Blood vessels are composed of tightly connected endothelial cells that are surrounded by a BM and other supporting cells, including smooth muscle cells and some contractile cells that wrap blood vessels named pericytes. When the endothelial cells detect the TAF gradient emanating from the tumor, they secrete MMPs that degrade the BM and ECM. The leading endothelial cells are sprout-tips and behind them, the other cells continue to divide and migrate. It can take on the order 10-21 days for new vessels to form and connect to the parent vessels. The final process is a neovasculature that provides the tumor with a direct supply of oxygen and nutrients.

2.2. Tumor Microenvironment

Egeblad's team [17] used a real-time microscopic imaging to show how cancer cells react to doxorubicin in the context of different microenvironments. "We were able to see clearly that the microenvironment contributes critically to drug response" Egeblad says "specifically via regulation of the permeability or leakiness of blood vessels running through and around the tumor, and also by impacting the local recruitment of inflammatory cells." Even though the gene in mice that encodes MMP9 enzyme,

which helps to regulate the permeability of blood vessels, had indicative leakier blood vessels, and this corresponds with a better response to doxorubicin. However, existing therapeutic inhibitors of MMP enzymes have failed in clinical trials, Egeblad notes: "Our data suggest that these or other drugs that affect vascular permeability could be used to achieve better responses to chemotherapies." This news gives us a route to follow in this section to understand the tumor itself and its microenvironment. Accordingly, we need to give some information about molecular and cell biology.

Tumor microenvironment is composed of a diversity of cell types such as endothelial cells, fibroblasts, immune cells which are interacted with malignant cells. An affluent source of growth factors and cytokines is satisfied by these stromal cells and they have a significant role in modulating existing connective tissue and depositing new matrix.

Fibroblasts are in particular significant, since *in vivo* and *in vitro*, they help to the formation and growth of tumors [18]. Fibroblasts located in the surrounding connective tissue are able to become activated, and myofibroblasts are these activated fibroblasts with smooth muscle differentiation. They do synthesis, deposition and remodeling of the underlying tissue matrix. Also, they produce many soluble paracrine growth factors that regulate cell proliferation, morphology, survival and death. They are not commonly seen in normal tissues while the number becomes abundant in the stroma of malignant cells.

Immune cells are attracted to the tumor site from the peripheral blood or lymphatic vasculature. They are responsible for detecting and destroying all particles that are foreign to the body, not necessarily tumor related. Tumor cells send antigens and this makes an alert in the immune system (e.g., cytotoxic T-lymphocytes CD8+ or macrophages) and they induce apoptosis in cells. However, there is a point which should be taken into account: Macrophages and other immune cell types are able to produce an array of pro-tumor factors which stimulate angiogenesis and facilitate metastasis.

Host stromal cells profoundly influence many steps of tumor progression such as tumor cell proliferation, invasion, angiogenesis, metastasis and even malignant transformation. Conversely, there is also a recent evidence that tumors induce changes in gene expression in the nearby stroma, which helps to sustain tumor growth. As an example, carcinomas may release signaling molecules that stimulate fibroblasts to secrete hepatocyte growth factor (HGF) which promotes tumor cell growth, decreases cell-cell adhesion and increases MMP secretion. Tumors may also alter gene expression in nearby noncancereous epithelial cells.

2.2.1. Extracellular Matrix (ECM)

The ECM is a complex composite material consisting of proteoglycan hydrogel connected with crosslinked collagen fibers which are less than 100 nm in diameter. It has a unique three dimensional architecture, since it is not tissue independent and its structural support permits sensing and transduction of biochemical and mechanical signals to cells [19].

The ECM provides biological context and structural support to the cells via a class of matrix receptors (integrins) that bind the ECM with some specificity. ECM consists of cross linked fibers which are collagen, elastin, fibronectin and laminin. We can itemize the differences between healthy tissues and tumor regarding the ECM properties:

(i) The organization and density of ECM fibers surrounding the normal epithelium differ from tumors.
(ii) The alignment and cross-linking of stromal fibers around tumors can be altered by both tumor-associated stromal fibroblasts and the invading tumor cells in such a way to facilitate tumor cell migration along the ECM fibers.
(iii) Elevated number of tissue rigidity influence molecular signals which cause malignant behaviour of tumor cells.

2.2.2. Interstitial Fluid (IF)

The interstitial space in the ECM is occupied by a fluid that is usually in motion and consists of a water solvent containing amino acids, sugars, fatty acids, hormones and salts as well as waste products from the cells. The differences between pressure in capillaries and in the interstitium (interstitial fluid gradient, IFP) cause the transcapillary flow of water and other molecules through the interstital space and the drainage into the lymph vessels that prevents a build-up of tissue fluid. The effects of antiangiogenic therapy on the levels of IFP and velocity are worked by Jain *et al.* [20]. They show that interstitial convection within the tumor may increase while fluid convection out of the tumor margin decreases. Decreasing convection of growth factors from the tumor margin into the peritumor tissue may reduce angiogenesis. Furthermore, decreased convective flow out of the tumor will likely decrease dissemination of cancer cells to lymph nodes. In all cases, the probability of lymphatic metastasis would be reduced.

2.2.3. Tumor Vasculature

Tumor vasculature provides necessary and sufficient amounts of nutrients and oxygen to the parenchymal cells and it removes waste products. However, the regions far from blood vessels are chronically hypoxic since tissue diffusion limit oxygen is 100-200 μm. Also, the existence of blood vessels does not mean tissue oxygenation is sufficient in tumors. It is experimented by high resolution intravital microscopy that there is no explicit relationship between blood flow rate and oxygen tension (pO_2). Moreover, one of the consequences of low extracellular pH is the abnormal microcirculation in the tumor. Both pO_2 and pH determine significantly tumor growth, metabolism, and response of tumor to therapies.

Oxygen is an important component of radiation therapy. Likewise, hypoxia and acidosis are indicators of the abnormal metabolic environment in tumors. It is observed that anaerobic glycolysis in hypoxic tumor cells results in a decreased microenvironmental pH. Exposure to hypoxia and/or acidic pH triggers tumor cells to be highly

Table 2.1. Vasculature of Solid tumors vs. Normal tissues.

	Tumor Tissue	**Normal Tissue**
Vessels	Leaky, dilated, tortuous and blood flow is heterogeneous	Well-organized, regulated and functional architecture.
Vasculature	Large inter-endothelial junctions, increased numbers of fenestrations, lack of normal basement membrane	Regular formations
Branches	Trifurcations, uneven diameters	Dichotomous branching

invasive and metastatic by inducing apoptosis in the surrounding normal epithelium. Hypoxia initializes the secretion of various angiogenic growth factors, including vascular endothelial growth factor (VEGF), angiopoietin, platelet derived growth factor. This plays a role for tumor invasion by giving invasive tumor cells a selective advantage over tumor cells that have not adapted to acidity, which contribute the ECM degradation (due to proteases released by apoptotic cells). Detailed analysis indicates that in low pH or oxygenated regions, tissue pH, but not pO_2 regulates VEGF promoter activity. Conversely, in hypoxic or neutral pH regions, tissue pO_2 and not pH regulates VEGF expressions. Combining these data together, one can propose that two microenvironment parameters in solid tumors drive angiogenic factors in opposite ways.

In solid tumors, IFP is increased by vascular hyperpermeability and deficiency of functional lymphatic vessels. These abnormalities build a physiological barrier to the delivery of therapeutic agents to tumors.

The underlying molecular mechanisms causing the abnormal vascular architecture are not well understood but one of the main ingredients is the imbalance of pro- and anti-angiogenic factors. Proliferating tumor cells generate solid (mechanical) stress that yield the compression in vessels of tumors. Moreover, the combination of both molecular and mechanical factors may render the tumor vasculature abnormal.

Extravasation of molecules from the bloodstream is realized by diffusion, convection and transcytosis which is the process by which various macromolecules are transported across the interior of a cell. Blood capillaries are well-known sites for transcytosis.

Diffusion is a key determinant of transvascular transport in tumors. The diffusive permeability of a molecule not only depends on its size, shape, charge and flexibility, but also the transvascular transport pathway influences it. It is remarkable that vascular permeability in solid tumors is generally higher than in various normal tissues.

Tumor blood flow is unevenly distributed. Moreover, it not only rises and falls with time but also it reverses its direction in some vessels so the areas with poor perfusion generally observed. The abnormal microenvironment structure is also delivered by the heterogeneity of tumor blood flow and this heterogeneity hinders the delivery and efficacy of therapeutic agents to tumors. Both animal and human tumors exhibit interstitial hypertension while IFP in normal tissues is around zero mmHg. The hydrostatic and oncotic pressures become almost equal between intravascular and extravascular spaces due to tumor vessels' perm selectivity deficiency resulting from the high vascular permeability. IFP is uniformly high throughout a tumor and it drops rapidly around the tumor boundary. This uniformly elevated IFP hinders the delivery of therapeutic agents both across the blood vessel wall and interstitium in tumors.

On the other hand, IF flows gradually out from the tumor periphery into the surrounding normal tissue carrying angiogenic, lymphangiogenic growth factors and/or metastasing tumor cells with it. The absence of functional lypmhatics is another reason of increased tumor IFP. In the established tumors, the drastic increase of IFP at the tumor boundary might be used to locate tumors during needle biopsy and ameliorate diagnosis of patients. A study of cervical cancer has depicted that increasing IFP can forecast poor outcome of radiation therapy.

Collagen remodeling in perivascular stroma have clinical benefits such as normalizing tumor vasculature, reduction in IFP and modulation of hydraulic conductivity

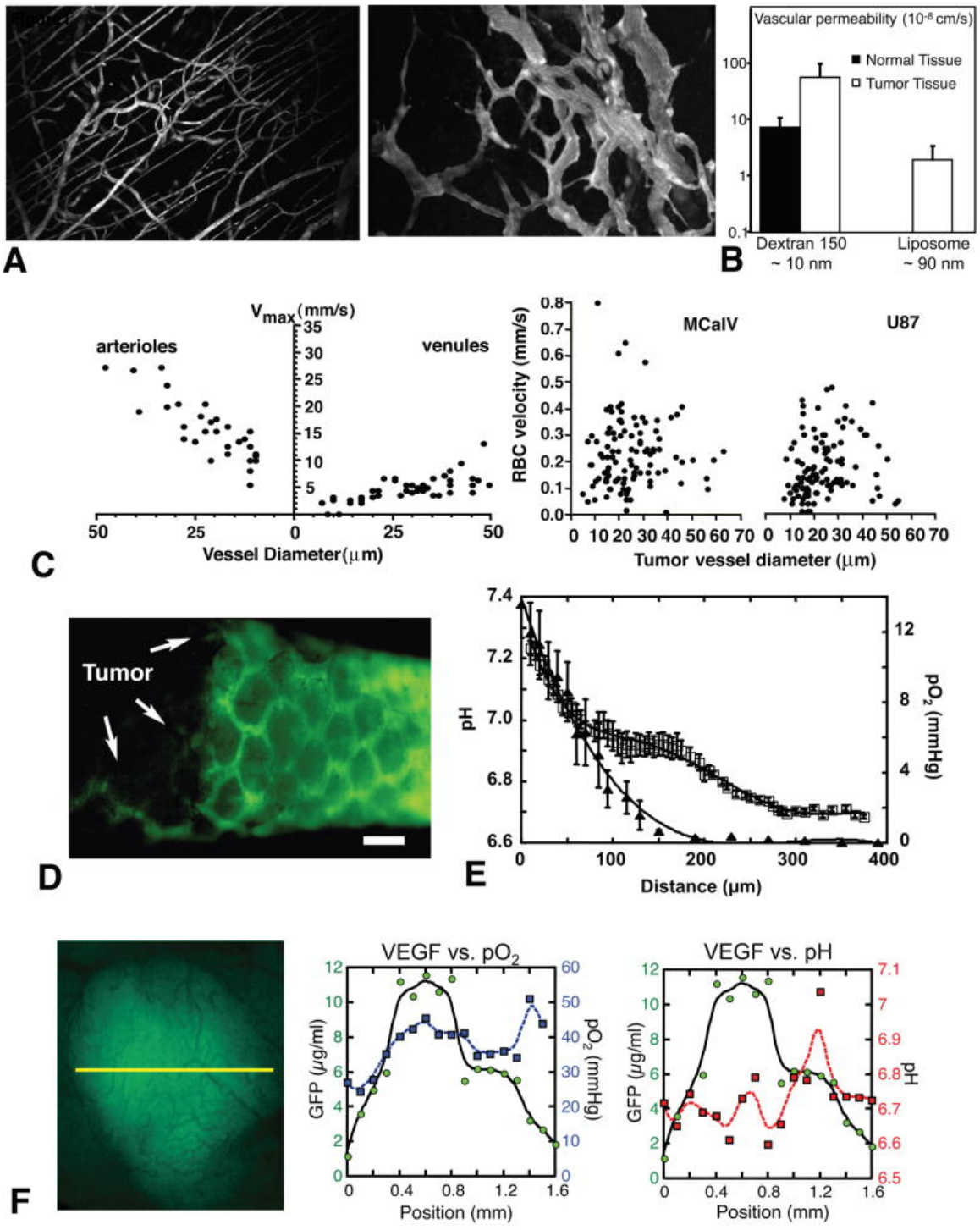

Figure 2.2. Vascular Permeability [4].

of the stroma and fluid balance. As a result of this, tumor perfusion and delivery of cytotoxic drugs in solid tumors might be improved [21].

As an example of normalization therapy, Bevacizumab (anti-VEGF antibody) and DC101 (anti-VEGF2 antibody) form some tumor vessels and remodel the remaining vasculature in human colon cancer and glioma as well as murine breast cancers resemble normal. They decrease IFP in breast and colon cancers and gliomas so pressure gradient across blood vessel wall as well as tumor interstitium is restored. Both Bevacizumab and DC101 improve tumor tissue oxygenation in human glioma and increase drug penetration in tumors. The radiation treatment and its efficiency are significantly improved when compared with anti-VEGF treatments.

Tumor hydraulic conductivity is strongly correlated with tissue hydration according to data reported for other soft tissues. The control mechanism of the rate of interstitial transport is satisfied by the tissue hydraulic conductivity and the diffusion coefficient which define the intrinsic convective and diffusive rate of the transport, respectively. It is also remarkable that the resistance to the water flow is lower in tumor than in normal tissues.

Hydraulic conductivity manages the interstitial fluid velocity along with the retardation factor which determines the interstitial convective rate of a solute. The retardation factor is a phenomenological parameter and depends on tissue hydration, structure, and molecular properties of a solute. Interstitial resistance to water and solute transport is attributed to the amount of proteoglycans. There exists a general correlation between fluid and solute transport resistance with the amount of glycosaminoglycans (GAGs) in the tissue [13].

2.2.4. Matrix Metalloproteinases (MMPs)

According to [22], matrix metalloproteinases (MMPs) can be defined as members of the metzincin group of proteases which share zinc-binding motif in their catalytic active site. In human body, 24 different MMPs are found which are ingredients of a

diverse family of enzymes. It is possible to group them under several common properties and domain structures:

(i) Collagenases (including MMP1-MMP8-MMP13),
(ii) Stromelysins (MMP3-MMP10),
(iii) Gelatinases (MMP2-MMP9),
(iv) Matrilysins (MMP7-MMP26),
(v) Membrane type MMPs (MT-MMPs),
(vi) Others.

One might find this fact interesting if she/he needs some details for classification: All MMPs are synthesised as pro-enzymes, except the membrane bound MT-MMPs, secreted into the extracellular environment. The structure of MT1-MMP contains the hemopexin domain (PEX) that is distinct from and additional to the catalytic domain. There is also a consensus among researches that MT1-MMP plays a significant role in tumor progression and metastasis. There are studies on MT1-MMP inhibitors by selectively targeting its PEX domain and repressing the protumorigenic function of MT1-MMPs [23].

The main properties of MMPs are briefly described in the article of Egeblad *et al.* [24]:

(i) MMPs regulate growth: Some of the growth-promoting signals are generated by MMPs.
(ii) MMPs regulate apoptosis: The escape from apoptosis allows survival even though there is no genetic stability, low levels of oxygen and nutrients, attacks from the immune system, anticancer treatment and detachment from the ECM which is a necessary step in metastasis.
(iii) MMPs regulate angiogenesis: They degrade the ECM, which allow endothelial cells to invade the tumor stroma.
(iv) MMPs play a role in invasion and metastasis: In experimental metastasis studies, the downregulation of MMP9 in lung cancer colonies of mice reduces the

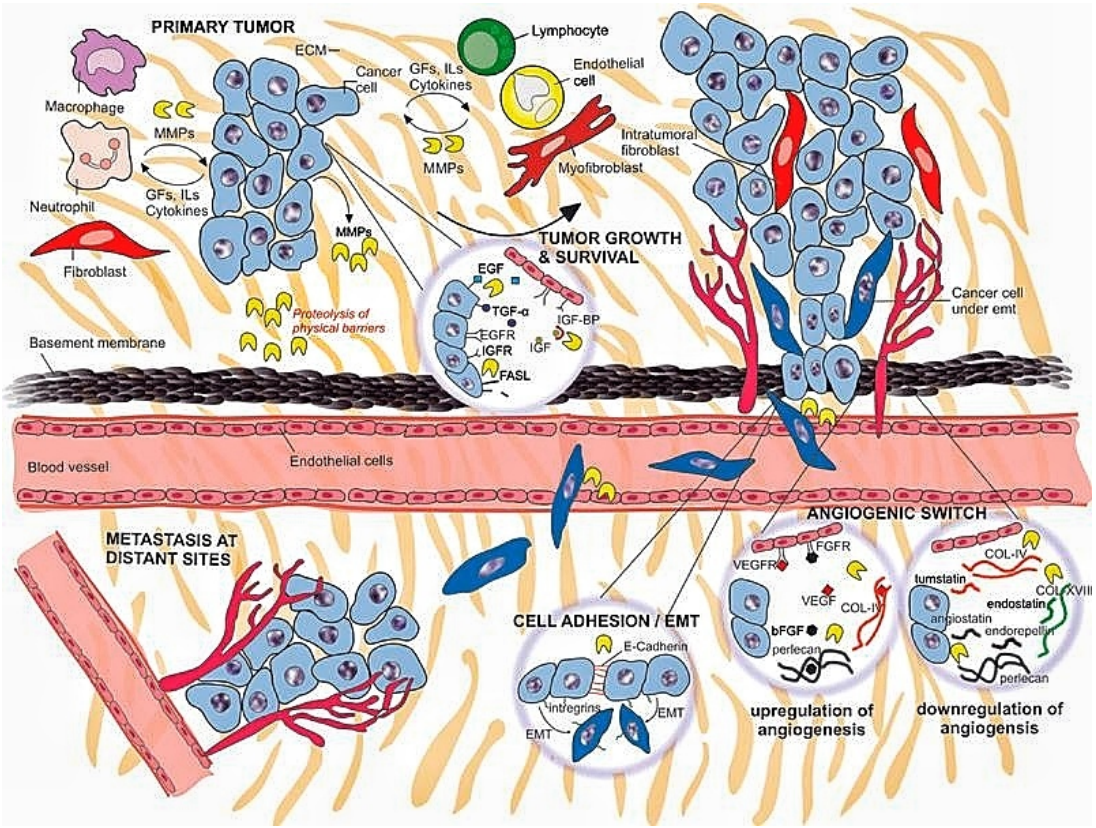

Figure 2.3. Pivotal Roles of MMPs in Cancer Progression [5].

formation.

(v) MMPs and the immune system response to cancer: They are involved in the escape mechanisms of cancer cells for immune surveillance.

However, in this thesis, we focus on some protective roles of MMPs which are often neglected in therapeutic methods and there is still not much success on clinical trials.

The researches have been triggered by the failure of MMP inhibitors in clinical trials. In [25], it is shown *in vivo* studies that, some types of MMPs like MMP-8 have controversial anti-tumor functions. Adding to these studies in mice, an experimental change of MMP-8 expression levels in human breast cancer cells has revealed that lack of MMP-8 in nonmetastatic cells increases its metastatic potential while its overexpression in metastatic cells substantially prevents this potential.

For MMP2, it is widely believed that it has a role in the invasion of brain tumor cells. However, this assumption is mainly based on *in vitro* studies. Trembley *et al.* [26] obtained that the tumors lacked of MMP2 have more invasive cells and less macrophages. Its vasculature was more sensitive to changes and fewer capillary sprouts supported it. In contrast, the tumors overexpressing MMP2 did not depict more histological difference than the controlled ones. The underlying reason might be explained with the fact that MMP2 does not result in vascular atypia (i.e., abnormality in a cell) in malignant brain tumors but a tissue repair response that tends to control the growth of these tumors is supported by it. So this research is a good example to inefficiency of a treatment for brain cancer against MMP2 inhibition.

Sounni *et al.* [21] investigated MT1-MMP activity in perivascular stroma and the regulation of vascular permeability *in vivo*. They also found that vascular leakage in both wild type and Collal mice is drastically raised by a broad spectrum MMP inhibitor GM6001. As a result, one can deduce a relation between steady state MMP activity and vascular leakage such as vessels become more susceptible to induced acute leakage under inhibition of steady-state MMP activity. Moreover, they observed that soluble MMPs not only play a role in the growth of pericyte recruitment and vessel maturation, they also ease pericyte migration and vessel coverage. Moreover, in experimental tumor models of melanoma and neuroblastom, it is observed that MMP inhibition reduces pericyte recruitment and decreases tumor vessel perfusion. MMPs release soluble factors hidden in the ECM and regulate vascular cell formation and maturation in several tumor models.

The reason of the inefficacy of broad spectrum MMP inhibitors might be ordered as the following [27]:

- Some MMPs have anti-tumor properties (e.g., MMP8 and MMP12). So it is suggested that the development of MMP inhibitors should be targeted at specific, well defined MMPs.

- It is observed that in early stages of cancer, MMP inhibitors are to more active

comparing to the late stage cancer.

- The significance of tumor microenvironment is proved by the examination of MMP expression in human tumor tissue sections. It is demonstrated that MMPs are mostly produced by recruited reactive stromal cells rather than the tumor cells themselves. Therefore, the cellular target for MMP inhibition is required to be more accurately defined.

- Some MMPs trigger tumor proliferation through ECM degradation which is mostly known but also they yield a split of many non ECM proteins. MMPs prevent apoptosis, regulate angiogenesis and innate immunity. The growth factors get rid of ECM by activation of MMPs. Cell migration depends on some chemical factors and they are also promoted by MMPs.

One of the responsibilities and challenges of biologists is to be able to differentiate the roles of MMPs that promote the tumor progression from those that are necessary for host defense, since preventing the latter will worsen the clinical outcomes as we discussed.

2.2.4.1. Why do MMPs play a critical role for drugs?. MMPs and their contribution to the cancer therapies are highly emergent concept and the contradictory results have been divided the researches into two groups. On one side, the articles, especially the ones coincide with the years of the discovery of MMPs, emphasize the properties of MMPs that facilitate tumor invasion and metastasis more than 30 years ago. On the other hand, new researches and clinical outcomes necessitate to look at the other side of the coin: MMPs have newly discovered biological roles as aforementioned. Hence, this question have become a new version of *"Cap ou pas cap?"* among cancer researchers: *"Target or Anti-target?"* That is why in this thesis, we try to capture new information and developments as much as possible. The article pressed in April 2013 by Dufour and Overall [28] supports our approach.

The first therapies related to MMPs were peptidomimetics inhibitors (e.g., Batimastat, BB94; Ilomastat, GM-6001) and second generation inhibitors (Marimastat, BB2516; Prinomastat, BAY12-9566). However, neither alone nor in combination with other used chemotherapeutic did not give positive results in patients.

With the failure of broad spectrum MMP inhibitors and observation of protective roles of some MMPs make them a candidate for drug anti-target. Drug anti-targets can be defined as:

Definition 2.1 (Drug Anti-Target [28])**.** *"A molecule or protein with essential or host protective roles in the normal state of a cell or tissue function. Inhibition of its activity results in clinically unwanted side effects and initiation or worsening of a disease."*

Consequently, the reason why MMPs play a critical role for drug development lies behind the difficulty of determining the balance between the target and anti-target characteristics of MMPs with current knowledge.

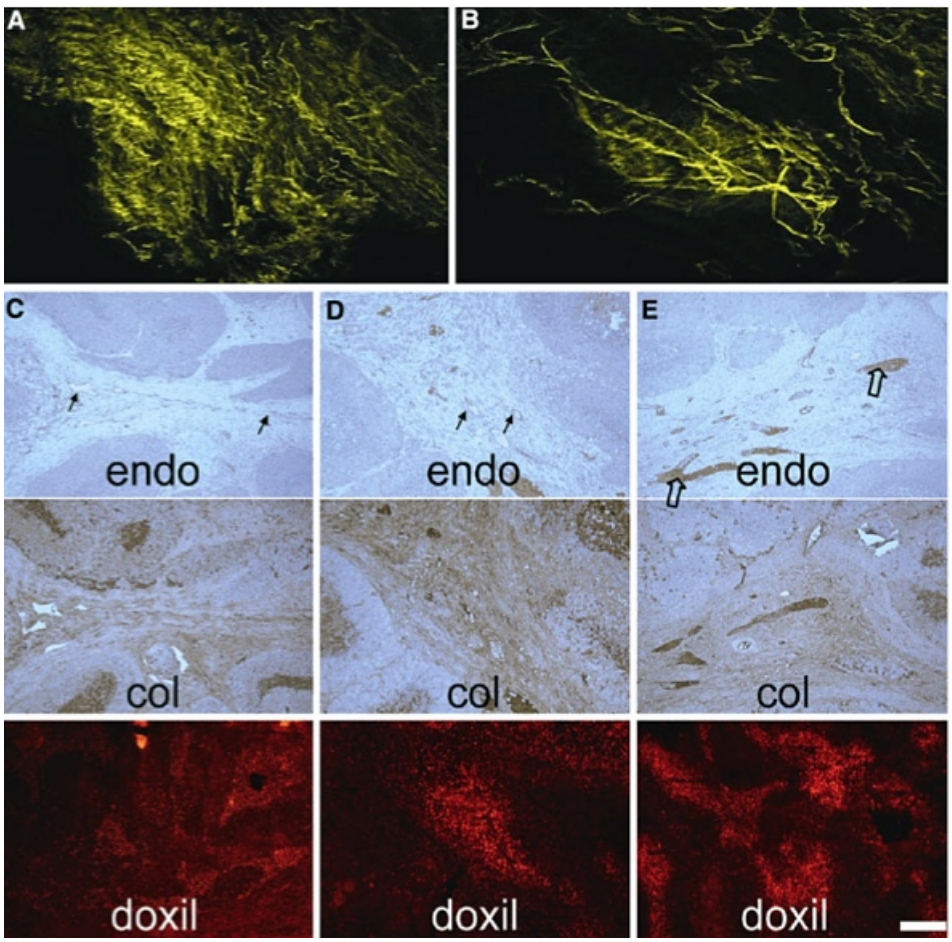

Figure 2.4. The Effect of Collagenase-2 Use on Collagen with Second-harmonic Generation Imaging and on Vessels (Endo, Brown), Collagens (Col, Brown), and Doxil Distribution (Doxil, Red) [6].

3. MODELING

In this chapter, we try to construct a mathematical model that describes the effect of MMP activation with the drug injection. To do this, some physical and physiological facts are needed. First, we explain our model with its assumptions and then give a derivation of mass balance equations. Then, we introduce some of important laws in transport phenomena which are *Starling's Law* and *Darcy's Law* describing the fluid flow in porous media.

3.1. Assumptions

Blood and lymph vessels are assumed to be uniformly distributed sources and sinks of fluid since intercapillary distance in tumors is about 300 μm. The mass balance equation for interstitial fluid having velocity $\mathbf{v_F}$ is:

$$\nabla \cdot (\phi_F \mathbf{v_F}) \quad = \quad \Gamma_{Fb} - \Gamma_{Fl}, \tag{3.1}$$

where ϕ_F is the volume fraction of interstitial fluid, Γ_{Fb} is the supply of fluid from blood vessels to the interstitial space and Γ_{Fl} is the drainage of fluid from the interstitial space into lymph vessels. The derivation of Equation 3.1 is discussed in the next Section 3.2.1. Comparing to the general mass balance equations, the time derivative of ϕ_F does not exist since the time scale in transport phenomena is much less than the tumor's time scale. For this reason, one of the model assumption is time independence of the physiological parameters used in the model [29].

In order to describe transvascular fluid flow, Starling's Law present two equations:

$$\Gamma_{Fb} = \lambda_{Fb}[P_0 - P - \sigma(\pi_c - \pi_i)] \tag{3.2}$$

and

$$\Gamma_{Fl} = \lambda_{Fl} P, \tag{3.3}$$

where λ_{Fb} and λ_{Fl} are hydraulic conductivities of blood and lymph vessel networks, respectively. P_0 is vascular fluid pressure, P is IFP, σ is the osmotic reflection coefficient, π_c and π_i are capillary and interstitial osmotic pressures, respectively. The hydraulic conductivities λ_{Fb} and λ_{Fl} are related to vessel wall hydraulic conductivities L_p and vessel surface densities by $\lambda_{Fb} = \lambda_{Fl} = L_p \frac{S}{V}$. In Equation 3.2, we have some assumptions. We neglect osmotic pressure contribution due to the high permeability of lymph vessels, (i.e., $\sigma \approx 0$) and we assume that lymph vessel pressure is 0 mmHg.

On the other hand, the flow of IF within the tissue is given by Darcy's Law:

$$q_F = -K \nabla P, \tag{3.4}$$

where q_F is the interstitial fluid flux (IFF) and K is the hydraulic conductivity of the tissue, respectively.

IFF is related to velocity of the IF ($\mathbf{v_F}$) by

$$q_F = \phi_F \mathbf{v_F}. \tag{3.5}$$

Combination of Equation 3.5 with Equations $3.1 - 4$ gives us:

$$\nabla \cdot (-K \nabla P) = \lambda_{Fb}[P_0 - P - \sigma(\pi_c - \pi_i)] - \lambda_{Fl} P. \tag{3.6}$$

Transport of the drug molecules is satisfied by the following convection-diffusion-

absorption equation:

$$\frac{\partial c}{\partial t} + \nabla \cdot (-D_c \nabla c) + \nabla \cdot (q_F \, c \, k_E) = \Gamma_{Fb}(1-\sigma)c_p + \lambda_d(c_p - c) - \Gamma_{Fl} \, c - \lambda_r \, c. \quad (3.7)$$

Here, c and c_p are the tissue and plasma drug concentrations, respectively. Moreover, D_c is the diffusion coefficient in the tissue, k_E is the retardation coefficient for transvascular convection, λ_d is the transvascular diffusion coefficient and λ_r is the decay rate of drug molecules. The right-hand side of Equation 3.7 might be interpreted as the extravasation of drug molecules by convection, by diffusion, uptake by the lymphatic vessels and biological decay of the drug molecules. One of the assumptions is continuous distribution of vascular network.

Plasma drug concentration c_p is in fact an exponential decay function such that $c_p(t) = c_0 e^{-kt}$ where k is a nonnegative number and c_0 is the maximum plasma concentration of the drug after injection, respectively. If we take natural logarithm of both sides of this equation, we get a line $\log(c_p(t)) = \log(c_0) - kt$. One may consider the half life $t_{1/2}$ of the drug concentration which can be computed easily as:

$$t_{1/2} = \frac{\log(c_p) - \log\left(\frac{c_p}{2}\right)}{k} \quad (3.8)$$

$$= \frac{\log 2}{k}. \quad (3.9)$$

Hence, the plasma drug concentration after injection can be written as:

$$c_p(t) = c_0 e^{-(\log 2)t/t_{1/2}} \quad \text{for} \quad t \geq 0. \quad (3.10)$$

Now, we try to impose some more conditions which is this thesis' main work. The usage of broad spectrum MMP inhibitors did not give successful results in clinical trials even though in vitro studies might have been positive therapeutic effects. We

approach from a different angle that has not done before in mathematical models by taking into account [16, 30–32]:

$$\frac{\partial M}{\partial t} + \nabla \cdot (-D_M \nabla M) = \lambda_{Md}(M_p - M) + \lambda_{Mn} n - \lambda_{Mr} M, \tag{3.11}$$

where M and M_p are the MMP concentrations in the tissue and plasma, respectively. D_M is the constant diffusion rate of MMP molecules in the tissue, n is the average tumor cell density and λ_{Mn} is the production rate of MMP molecules by tumor cells, λ_{Md} and λ_{Mr} are the transvascular diffusion and decay rates of MMP molecules, respectively. It has been found that interstitial hydraulic conductivity is inversely correlated with collagen and glycosaminoglycan content and IFP [31]. Moreover, remodeling of ECM in tumors by collagenases has been successful for the decreasing levels of IFP and it has improved the accumulation of liposomal doxorubicin in tumors [6]. Type I collagenase in human is in fact known as matrix metalloproteinase-1 (MMP1). Mok [16] has been examined the relation between interstitial hydraulic conductivity with MMP1 and MMP8, and he concluded these matrix metalloproteinases are effective to increase the hydraulic conductivity which yields lower IFP, and this becomes beneficial to the distribution of oncolytic virus (HSV) in the tumor tissue. Likewise, M. Kato *et al.* [31] have found that collagenase-1 treatment improved the accumulation and gene expression in tumors after intravenous injection of lipoplex. Regarding these studies, we assume the impact of matrix metalloproteinase concentration on hydraulic conductivity as:

$$K = K_0 + D_E M^{\alpha_M} \tag{3.12}$$

where K_0 is the hydraulic conductivity without MMP expression and D_E is the effective diffusion coefficient of MMPs in tumors, respectively. We assume K and M are linearly proportional not to make the system too complicated.

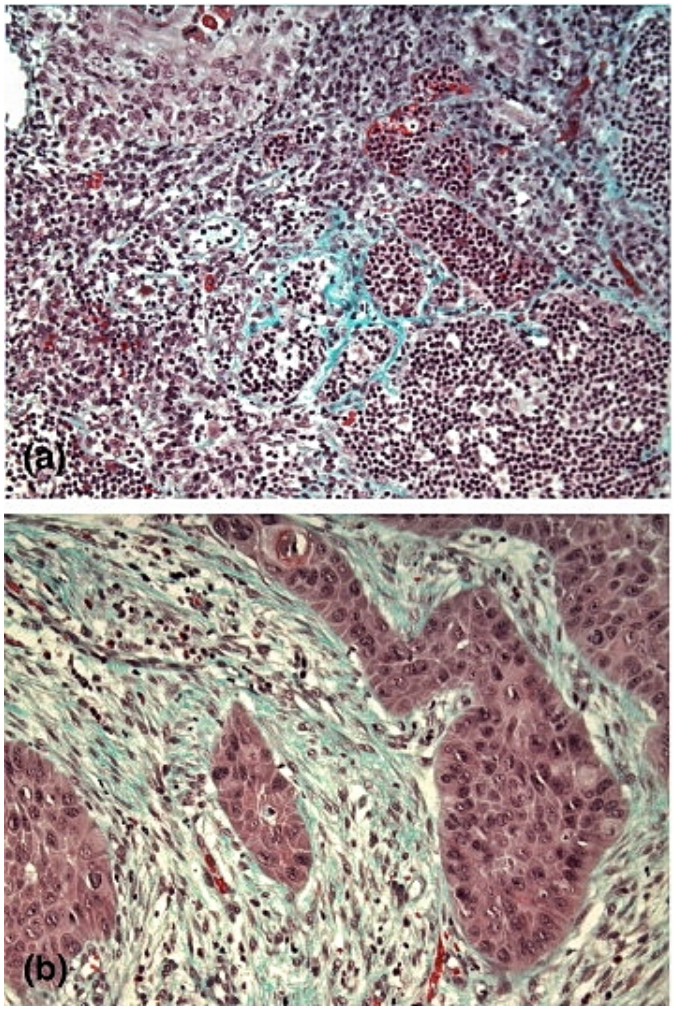

Figure 3.1. Effects of Hydraulic Conductivity in Two Different Tumors. In (a) Tumor has Low Malignant Cell Density, Minimal Interstitial Collagen and High $K = 3.7 \times 10^{-7}\ cm^2/mmHg.s$. Conversely, the Tumor in (b) has Larger Cell Density, More Collagen and Lower $K = 5.7 \times 10^{-9}\ cm^2/mmHg.s$ [7].

One of the reasons why some chemotherapy methods do not give positive results on patients might be explained by the heterogeneous distribution of drug within solid tumors [32]. Overcoming these barriers and obtaining a uniform delivery are the key issues for scientists. We define some quantities which measure total tumor exposure Φ_e and heterogeneity of drug distribution Φ_h by:

$$\Phi_e = \frac{1}{t_T c_0} \int_0^{t_T} dt \, \langle c \rangle_{\Omega_T} \,, \tag{3.13}$$

$$\Phi_h = \frac{1}{t_T c_0} \int_0^{t_T} dt \, \left\langle (c - \langle c \rangle_{\Omega_T})^2 \right\rangle_{\Omega_T}^{1/2} . \tag{3.14}$$

Here, $\langle . \rangle_{\Omega_T} = \frac{1}{V_T} \int_{\Omega_T} d^3\mathbf{x}(.)$ is the average integral over the tumor domain V_T where $d^n\mathbf{x} = \prod_{i=1}^{n} dx_i$ for a point $\mathbf{x} = \{x_1, x_2, \ldots, x_n\}$ in $\mathbb{R}^n$, describes a volume element and t_T is the time interval that the efficiency of the therapy is evaluated.

For tumor domain and boundary conditions, we consider a spherically symmetric tumor embedded in normal tissue. Problem parameters are given by assuming uniform and distinct values within the tumor domain Ω_T and normal tissue domain Ω_N. At the boundary between the tumor and normal tissue, we assume mass continuity relations for the interstitial fluid and zero flux of MMPs across the boundary:

$$\left[-K \frac{\partial P}{\partial r} \right]_{r=R_0} = 0, \tag{3.15}$$

$$\left[-D \frac{\partial c}{\partial r} - K \frac{\partial P}{\partial r} (1 - \sigma) c \right]_{r=R_0} = 0 \tag{3.16}$$

$$\left[\frac{\partial M}{\partial \nu} \right]_{r=R_0} = 0, \tag{3.17}$$

where R_0 is the tumor radius. Symmetric boundary conditions are valid at the tumor

center and far field:

$$\left.\frac{\partial P}{\partial r}\right|_{r=0,R^{\infty}} = 0, \tag{3.18}$$

$$\left.\frac{\partial c}{\partial r}\right|_{r=0,R^{\infty}} = 0, \tag{3.19}$$

$$\left.\frac{\partial M}{\partial r}\right|_{r=0,R^{\infty}} = 0. \tag{3.20}$$

3.2. Derivation of PDEs

3.2.1. Balance Equations, Conservation Laws and Reynolds' Transport Theorem

Derivation of the balance equations for a fluid is a necessary step to construct models in transport phenomena. In this section, we derive conservation of mass equations and general balance law equations. First, we mention *Reynolds' Tranport Theorem* and *Divergence Theorem* and then discuss the possibilities of the versions of a control volume that depend on the kinematics of the surface covering. We assume that $V(t)$ is an arbitrary control volume with a closed boundary $\partial V(t)$ where its unit outward normal vector is $\mathbf{n}$. Let $\mathbf{v}$ be the local average velocity of the continuum and $\mathbf{v}'$ be the velocity of the surface of the control volume. We mainly follow Preziosi's work [33] and the lecture notes of Prof. Higgins in a detailed way [34].

- Fixed Control Volumes: The control volume is fixed in physical space, (i.e., $\mathbf{v}' = 0$). In this case, there might be a mass flux through the boundaries of the control surface and this defines an *open system.*
- Material Control Volumes: The control volume does not allow a mass flux through the surface so that $\mathbf{v}' = \mathbf{v}$. We denote this as $V_m(t)$ and its boundary surface as $\partial V_m(t)$. They are also called Lagrangian control volumes and useful to derive the balance law equations.
- Moving Control Volumes: This control volume is the most suitable case in real

life. In general, $\mathbf{v}'$ does not have to be the same with $\mathbf{v}$ and also $\mathbf{v}' \neq 0$ on the control surface. There is a mass flux passing through the control surface. We denote moving control volumes by $V(t)$ and its control surface by $\partial V(t)$ as we defined above.

Now, we present the Reynolds' Transport Theorem which is a three dimensional version of Leibniz' rule for differentiating one dimension integrals.

Theorem 3.1. *Let $\phi(\mathbf{x}, t)$ be a scalar function defined per unit volume. The total amount of ϕ on the material control volume $V_m(t)$ is defined as:*

$$\Phi(t) := \int_{V_m(t)} \phi(\mathbf{x}, t)\, dV. \tag{3.21}$$

The rate of change of the total amount Φ with respect to time is

$$\frac{d}{dt}\Phi(t) := \frac{d}{dt}\int_{V_m(t)} \phi(\mathbf{x}, t)\, dV \tag{3.22}$$

$$= \int_{V_m(t)} \frac{\partial \phi}{\partial t}\, dV + \int_{\partial V_m(t)} \phi\, \mathbf{v} \cdot \mathbf{n}\, dS. \tag{3.23}$$

If we have an arbitrary control volume $V(t)$ with surface $\partial V(t)$, then the surface moves with velocity $\mathbf{v}'$ and the rate of change of Φ becomes:

$$\frac{d}{dt}\Phi(t) := \frac{d}{dt}\int_{V(t)} \phi(\mathbf{x}, t)\, dV \tag{3.24}$$

$$= \int_{V(t)} \frac{\partial \phi}{\partial t}\, dV + \int_{\partial V(t)} \phi \mathbf{v}' \cdot \mathbf{n}\, dS. \tag{3.25}$$

We can consider the general form of balance equations as:

Time rate of change	= Net rate of mass flow	+ net rate at which mass
of mass within $V_m(t)$	into $V_m(t)$ through $\partial V_m(t)$	is created within $V_m(t)$

or they can be written as:

$$\frac{d}{dt}\int_{V_m(t)} \rho\,\phi\; dV = -\int_{\partial V_m(t)} j\cdot\mathbf{n}\; dS + \int_{V_m(t)} \rho\,\Gamma\; dV, \tag{3.26}$$

where ρ is the continuum density and Γ is the rate at which mass is created per unit volume within the material control volume, respectively. Since the flux vector j points outward from the control volume, we put a negative sign to indicate that there is an influx.

If $\rho(\mathbf{x},t)$ denotes the local density of the continuum, then the change of total mass with respect to time depends on the source term Γ and if it does not exist then the change is zero. The reason is that we take material control volumes; put differently, there is no mass travels through the surface $\partial V_m(t)$ since $\mathbf{v}=\mathbf{v}'$. Denoting $M(t)$ as the total mass of continuum, we can write:

$$M(t) := \int_{V_m(t)} \rho(\mathbf{x},t)\; dV, \tag{3.27}$$

$$\frac{dM}{dt} = \int_{V_m(t)} \rho\,\Gamma\; dV. \tag{3.28}$$

By applying Theorem 3.1 to Equation 3.28, we get:

$$\int_{V_m(t)} \frac{\partial\rho}{\partial t}\; dV + \int_{\partial V_m(t)} \rho\,\mathbf{v}\cdot\mathbf{n}\; dS = \int_{V_m(t)} \rho\,\Gamma\; dV. \tag{3.29}$$

Now, Divergence Theorem comes on the scene:

Theorem 3.2. *Let W be a symmetric elementary region in space and ∂W denotes the oriented closed surface that envelopes W. Let $\mathbf{F}$ be a smooth vector field defined on W. Then*

$$\int_W (\nabla\cdot\mathbf{F})\; dV = \int_{\partial W} (\mathbf{F}\cdot\mathbf{n})\; dS \tag{3.30}$$

where an elementary region in three dimensional space is obtained by restricting one of the variables to be between two functions of the remaining variables, the domains of these functions being an elementary region in the plane. If an elementary region can be simultaneously described in all three ways, it is called symmetric elementary region.

Using Divergence Theorem 3.2, we can arrange Equation 3.29 as follows:

$$0 = \frac{d}{dt}\int_{V_m(t)} \rho(\mathbf{x},t)\, dV - \int_{V_m(t)} \rho\,\Gamma\, dV \tag{3.31}$$

$$= \int_{V_m(t)} \frac{\partial \rho}{\partial t} + \nabla\cdot(\rho\,\mathbf{v}) - \rho\,\Gamma\, dV. \tag{3.32}$$

Since the above equation is true for any material control volume $V_m(t)$, this can be true only when

$$\frac{\partial \rho}{\partial t} + \nabla\cdot(\rho\,\mathbf{v}) - \rho\,\Gamma = 0. \tag{3.33}$$

The above derivation is the differentiation form of the conservation of mass and sometimes can be called as *continuity equation.*

Even though the continuity equation has many applications and it is one of the equations in the *Navier-Stokes equations* which use conservation of mass, conservation of linear momentum and incompressibility of fluids, the control volume does not have to be material control volume. We now demonstrate the validity of continuity equations by taking an arbitrary control volume $V(t)$.

Since $\mathbf{v} \neq \mathbf{v}'$, the mass can be travelled across the boundary $\partial V(t)$. Notice that the surface element dS moves with velocity $\mathbf{v}'$ while the mass travels with an average

velocity $\mathbf{v}$ so the net mass influx across the surface should be with the relative velocity:

$$\{\text{The net mass influx across} \quad \partial V(t)\} = -\int_{\partial V(t)} \rho\,(\mathbf{v} - \mathbf{v}') \cdot \mathbf{n}\; dS. \tag{3.34}$$

Therefore, we obtain a specialized version of Equation 3.26 by taking $\phi = 1$:

$$\frac{d}{dt}\int_{V(t)} \rho\, dV = -\int_{\partial V(t)} \rho\,(\mathbf{v} - \mathbf{v}') \cdot \mathbf{n}\; dS + \int_{V(t)} \rho\,\Gamma\; dV. \tag{3.35}$$

Combining the last equation with Divergence and Reynolds' Transport theorems, we obtain:

$$0 = \int_{V(t)} \left(\frac{\partial \rho}{\partial t} + \nabla \cdot (\rho\,\mathbf{v}') + \nabla \cdot \rho\,(\mathbf{v} - \mathbf{v}') - \rho\,\Gamma \right)\; dV. \tag{3.36}$$

Since $\nabla \cdot (\rho\,\mathbf{v}') + \nabla \cdot \rho\,(\mathbf{v} - \mathbf{v}') = \nabla \cdot \rho\,(\mathbf{v})$ and the control volume $V(t)$ on which we take the integral is arbitrary, the integrand above must be zero, which gives again the continuity equation.

3.2.2. Starling's and Darcy's Laws

Transvascular fluid flow occurs by the existence of osmotic pressure. The osmotic pressure can be defined as the pressure which must be applied to a solution in order to satisfy the equilibrium with pure solvent and solvent of the solution. That pressure is proportional to the concentration of the solute. Fluid flow in pure solutions or porous media can be pushed by shear stresses or pressure gradients. Even though the shear stresses might not contribute to the fluid flow due to the negligible thickness of the membrane, the hydrostatic and osmotic pressures differences must be considered for a *semipermeable* membrane.

The effect of an osmotic pressure difference on fluid flow across a microvessel wall had been observed firstly by Starling in 1896. He found that the rate of fluid flow across the microvessel wall is proportional to the hydrostatic pressure difference Δp minus the osmotic pressure difference $\Delta\pi$, which is:

$$J_v = L_p S(\Delta p - \sigma_s \Delta\pi). \tag{3.37}$$

The coefficients can be defined as the following: L_p is the hydraulic conductivity of the vessel wall, S is the surface area of the endothelium, σ_s is the osmotic reflection coefficient where $0 \leq \sigma_s \leq 1$. This coefficient must be taken into account when microvessel wall is permeable (e.g., albumin). When this coefficient gets closer to 1, it can be read as the vessel wall is permeable and increasing permeability yields σ_s close to 0. Also, in the body, the osmotic pressure difference across a microvessel wall is driven by the plasma proteins and for continuous capillaries, it is generally experimented that $0.7 \leq \sigma_s \leq 0.9$.

Fluid flow for porous media can be explained by *Darcy' law* and it says basically that fluid flow rate is proportional to the pressure gradient. Even though this was an empirical relation discovered by Darcy, it was also theoretically derived by the mechanical analysis of fluid flow. Darcy's law is not valid for non-Newtonian fluids, for Newtonian liquids at high velocity and for gases having very low and very high velocities. The concept of Newtonian fluids is beyond our scope; however, high-molecular-weight polymers, synovial fluid, slurries and suspensions might be some examples for non-Newtonian fluids. Since interstitium of biological tissues behave like Newtonian fluids, Darcy's law can be widely used to investigate interstitial fluid flow.

In a homogeneous and isotropic (i.e., the pressure at a given point is the same in

all directions) medium, Darcy's law can be written as:

$$\mathbf{v} = -K\nabla p, \tag{3.38}$$

where ∇p is the gradient of the hydrostatic pressure and K is a constant defined as the hydraulic conductivity. If the medium is non-homogeneous and nonisotropic, then K is exposed to the location in the medium [35].

4. SIMULATION

In a modeling, each step belongs to different methods and tools while they serve a unique aim at the end: A valid result for real phenomena. This chapter is one of the most significant levels for modeling which is a simulation process. Simulation is roughly the solution of the PDEs that is presented for the model and it requires a successful interaction between mathematics and computer sciences. Numerical differentiation can be handled via different approaches, shooting method, finite difference method, finite element method (FEM) and some other more improved techniques. In our model, we implement finite element method due to some specific reasons. The first one is the program COMSOL Multiphysics that we use for simulation drives finite element method inside implicitly. Also it has an ability to handle with problems defined on complex geometries. However, the second reason is much more related to our work: *Optical Imaging.* My supervisor and his research group work not only on theoretical modeling and its simulation but also photoacustic imaging (http://www.phys.boun.edu.tr/ burcin/research.html).

There exists plenty of optical and biomedical imaging techniques in order to measure the internal structure of objects, each of them works under different principles and the way from which they capture information. For instance, computed tomography (CT) uses X-rays to measure and image a cross-sectional slice of an internal organ of the human body. This measurement can be achieved by *scattering of electromagnetic waves* from the object. On the other hand, magnetic resonance imaging (MRI) measures the radio waves when the magnetic field to which the organ subject is suddenly switched whereas Ultrasound imaging uses ultrasonic waves and its application area is mammography. Nonetheless, photoacoustic imaging is developed based on the photoacoustic effect where non-ionizing laser pulses are delivered into biological tissues. Recent researches reveal that *in vivo* tumor angiogenesis monitoring, blood oxygenation mapping, functional brain imaging and skin melanoma detection can be obtained by photoacoustic imaging [36].

What is the relation between a mathematical theory of numerically solving ordinary and partial differential equations and optical imaging? The answer lies in the theory of *inverse problems.* In those inverse problems, the aim is to reconstruct some of the physical parameters in the differential equation inside spatial domains from partial measurements of the solutions on the boundaries of the domains and in fact the image at the end is the solution of the inverse problems [37]. However, this process is not easily handled due to the existence of an unknown number of small irregularities in these physical parameters at unknown locations (e.g., the existence of tumors) and the required resolution for clinical usage needs meshes which yield a huge problem with so many unknowns. That is a good reason why the mathematicians collaborate with computer scientists, and vice versa. The finite element method (FEM) has been used over the last decade and an obvious success in reducing the complexity of problems in the solution of partial differential equation can be seen [38].

With this motivation, we give an introduction to the theory of finite element methods and then try to attempt an application for our model.

4.1. Finite Element Method

4.1.1. Galerkin method

In this section, we introduce the theory of FEM and mainly follow Kress' book [39] and the lecture notes of Ir. A. Segal [40]. We are concerned with the solution of the operator equation

$$Au = f$$

for a given bounded linear operator $A : X \to X$ on a Hilbert Space X and an element $f \in X$. For an element $u \in X$, we have

$$u \quad \text{solves} \quad Au = f \quad \text{if and only if} \quad \langle v, Au\rangle = \langle v, f\rangle \quad \text{for all} \quad v \in X, \tag{4.1}$$

where $\langle ., . \rangle$ defines an inner product (real or complex valued) on X.

The Galerkin Method is mainly based on this observation: Given a finite dimensional subspace X_n of X, Equation 4.1 can be approximately solved by an element $u_n \in X_n$ such that

$$\langle v, Au_n \rangle = \langle v, f \rangle \quad \text{for all} \quad v \in X_n. \tag{4.2}$$

Here u_n is called the *Galerkin solution* or *Galerkin approximation.*

If $w_1, w_2, \ldots, w_n$ is a basis for X_n, then for

$$u_n = \sum_{i=1}^{n} \alpha_i w_i, \tag{4.3}$$

the Galerkin Equations (4.2) are equivalent to the system of linear equations

$$\sum_{i=1}^{n} \overline{\alpha_i} \langle w_j, Aw_i \rangle = \langle w_j, f \rangle \tag{4.4}$$

for $j = 1, 2, \ldots, n$ and by unique solvability of Galerkin equations Theorem A.2, this linear system of equations is uniquely solvable.

Now, we consider Galerkin Method to determine $u \in X$ for the equation $S(u, v) = F(v)$ for all $v \in X$, where $S : X \times X \to \mathbb{C}$ is bounded, strictly coercive sesquilinear function (see Defns. A.2-A.3) and $F : X \to \mathbb{C}$ is a bounded linear functional on a Hilbert Space X. By Lax-Milgram Lemma A.4 and Riesz's theorem A.1, Galerkin equation hereby turns into

$$S(v, u_n) = \langle v, Au_n \rangle = \langle v, f \rangle = F(v) \tag{4.5}$$

for all $v \in X_n$. Accordingly, this equation is equivalent to the system of linear equations,

if $w_1, w_2, \ldots, w_n$ is a basis for X_n,

$$\sum_{i=1}^{n} \overline{\alpha_i} S(w_j, w_i) = F(w_j) \tag{4.6}$$

for $j = 1, 2, \ldots, n$ and $u_n = \sum_{i=1}^{n} \alpha_i w_i$.

The finite element method consists of an application of Galerkin method to the weak formulation of differential equations by spline spaces.

Definition 4.1. *A function $c \in H_0^2(\Omega)$ (see Theorem A.6) is called a weak solution to the reaction-diffusion equations provided:*

$$-\nabla \cdot (A \nabla c) + \beta c = f \quad on \quad \Omega, \tag{4.7}$$

$$c = g_1 \quad on \quad \Gamma_1, \tag{4.8}$$

$$A \nabla c \cdot \mathbf{n} = g_2 \quad on \quad \Gamma_2, \tag{4.9}$$

$$\sigma\, c + A \nabla c \cdot \mathbf{n} = g_3 \quad on \quad \Gamma_3 \quad (\sigma \geq 0), \tag{4.10}$$

where the boundary Γ is divided into three parts Γ_1, Γ_2 and Γ_3 provided that

$$S(v, c) = F(v) \quad for\ all \quad v \in C^2(\Omega) \quad with \quad v = 0 \quad at \quad \Gamma_1. \tag{4.11}$$

The explicit weak formulation of Equation 4.7 can be derived via integrating the equation over its domain Ω:

$$\int_\Omega (-\nabla \cdot (A \nabla c) + \beta\, c)\, v\, d\Omega = \int_\Omega f\, v\, d\Omega. \tag{4.12}$$

Notice that,

$$\nabla \cdot (v A \nabla c) = \nabla v \cdot A \nabla c + v \nabla \cdot (A \nabla c). \tag{4.13}$$

Recall Divergence Theorem **??** and extracting $v\nabla \cdot (A\nabla c)$ from Equation 4.13, we get:

$$\int_\Omega v(\nabla \cdot (A\nabla c)\, d\Omega = -\int_\Omega \nabla v \cdot A\nabla c\, d\Omega + \int_\Gamma v\, A\nabla c \cdot \mathbf{n}\, d\Gamma. \tag{4.14}$$

Hence, Equation 4.12 can be written as:

$$\begin{aligned}\int_\Omega (A\nabla c \cdot \nabla v + \beta\, c\, v)\, d\Omega = &-\int_{\Gamma_3} \sigma\, c\, v\, d\Gamma + \int_\Omega f\, v\, d\Omega \\ &+ \int_{\Gamma_2} g_2\, v\, d\Gamma + \int_{\Gamma_3} g_3\, v\, d\Gamma,\end{aligned} \tag{4.15}$$

where $v = 0$ on Γ_1.

Galerkin Equations (4.2) for the solution c can be written as:

$$\begin{aligned}\int_\Omega (A\nabla c_n \cdot \nabla w_i + \beta\, c_n\, w_i)\, d\Omega = &-\int_{\Gamma_3} \sigma\, c_n\, w_i\, d\Gamma + \int_\Omega f\, w_i\, d\Omega \\ &+ \int_{\Gamma_2} g_2\, w_i\, d\Gamma + \int_{\Gamma_3} g_3\, w_i\, d\Gamma.\end{aligned} \tag{4.16}$$

If we write

$$c_n = \sum_{i=1}^{n} c_i w_i + c_0, \tag{4.17}$$

where the function c_0 is chosen so that

$$c_0 = g \quad \text{at} \quad \Gamma_1, \tag{4.18}$$

$$w_i = 0 \quad \text{at} \quad \Gamma_1 \tag{4.19}$$

and if we put $v = w_i$ for $i = 1, 2, \ldots, n$ into Equation 4.15, in fact we obtain n equations with n unknowns (c_i's for $i = 1, 2, \ldots, n$). So putting $c_n = \sum_{i=1}^{n} c_i w_i + c_0$ into Equation

4.16:

$$\sum_{j=1}^{n} c_j \left[\int_\Omega (A\nabla w_j \cdot \nabla w_i + \beta\, w_j\, w_i)\, d\Omega + \int_{\Gamma_3} \sigma\, w_j\, w_i\, d\Gamma \right]$$
$$= \int_\Omega f\, w_i\, d\Omega + \int_{\Gamma_2} g_2\, w_i\, d\Gamma + \int_{\Gamma_3} g_3\, w_i\, d\Gamma$$
$$- \int_\Omega (A\nabla c_0 \cdot \nabla w_i + \beta\, c_0\, w_i)\, d\Omega. \tag{4.20}$$

As a result, we might consider Equation 4.20 as a matrix equation:

$$\mathbf{Sc} = \mathbf{F} \tag{4.21}$$

$$\tag{4.22}$$

or

$$S(v, c) = F(v), \tag{4.23}$$
$$S(v, c) = \int_\Omega (A\nabla c \cdot \nabla v + \beta\, c\, v)\, d\Omega, + \int_{\Gamma_3} \sigma\, v\, c\, d\Gamma \tag{4.24}$$
$$F(v) = \int_\Omega f\, v\, d\Omega + \int_{\Gamma_2} g_2\, v\, d\Gamma + \int_{\Gamma_3} g_3\, v\, d\Gamma$$
$$- \int_\Omega (A\nabla c_0 \cdot \nabla v + \beta\, c_0\, v)\, d\Omega. \tag{4.25}$$

To write explicitly,

$$S(w_i, w_j) = \int_\Omega (A\nabla w_j \cdot \nabla w_i + \beta\, w_j\, w_i)\, d\Omega, + \int_{\Gamma_3} \sigma\, w_j\, w_i\, d\Gamma \tag{4.26}$$
$$F(w_i) = \int_\Omega f\, w_i\, d\Omega + \int_{\Gamma_2} g_2\, w_i\, d\Gamma + \int_{\Gamma_3} g_3\, w_i\, d\Gamma$$
$$- \int_\Omega (A\nabla c_0 \cdot \nabla w_i + \beta\, c_0\, w_i)\, d\Omega. \tag{4.27}$$

Application of FEM requires subdivision of our domain Ω into simple elements. For instance, intervals for $\mathbb{R}$, triangles or quadrilaterals for $\mathbb{R}^2$ and tetrahedra or hexahedra are most suitable choices for simple elements. This finite subdivision process

is called finite element mesh. After then, we define finite number of points in these elements (i.e., grid points) so that the unknown functions are approximated by polynomials with lower degrees. If we work in $\mathbb{R}$, considering linear splines as basis functions might be a suitable choice for simplicity. These splines behave linear on each element and at grid points they become 0 or 1. More explicitly, if we divide an interval $[a, b]$ into $n \in \mathbb{N}$ points with $x_j = a + (j-1)h$ for $j = 1, 2, \ldots, n$ and the step size $h = \frac{b-a}{n-1}$:

$$w_k(x) = \begin{cases} \frac{1}{h}(x - x_{k-1}), & x \in [x_{k-1}, x_k], \\ \frac{1}{h}(x_{k+1} - x), & x \in [x_k, x_{k+1}], \\ 0, & x \notin [x_{k-1}, x_{k+1}]. \end{cases}$$

The integrals over Ω in Eqs. (4.26) can be evaluated over the mesh elements, that is:

$$\int_\Omega (A\nabla w_j \cdot \nabla w_i + \beta\, w_j\, w_i)\, d\Omega = \sum_{k=1}^{n_e} \int_{\Omega^{e_k}} (A\nabla w_j \cdot \nabla w_i + \beta\, w_j\, w_i)\, d\Omega, \tag{4.28}$$

$$\int_\Omega (A\nabla c_0 \cdot \nabla w_i + \beta\, c_0\, w_i)\, d\Omega = \sum_{k=1}^{n_e} \int_{\Omega^{e_k}} \int_\Omega (A\nabla c_0 \cdot \nabla w_i + \beta\, c_0\, w_i)\, d\Omega, \tag{4.29}$$

and

$$\int_\Omega f\, w_i\, d\Omega = \sum_{k=1}^{n_e} \int_{\Omega^{e_k}} f\, w_i\, d\Omega \tag{4.30}$$

where n_e denotes to the number of the mesh elements and Ω^{e_k} to the area of element e_k, respectively.

For a specific element Ω^{e_k}, only the basis functions corresponding to grid points in this element do not vanish so it is sufficient to evaluate nonzero integrals over this element.

Similarly, the integrals over the boundary Γ we assume that the boundary is identical to the outer boundary of the elements. Thus, we obtain:

$$\int_{\Gamma_3} \sigma\, w_j\, w_i\, d\Gamma = \sum_{k=1}^{n_{e^{\Gamma_3}}} \int_{\Gamma_3^{e_k}} \sigma\, w_j\, w_i\, d\Gamma, \tag{4.31}$$

$$\int_{\Gamma_2} g_2\, w_i\, d\Gamma = \sum_{k=1}^{n_{e^{\Gamma_2}}} \int_{\Gamma_2^{e_k}} g_2\, w_i\, d\Gamma, \tag{4.32}$$

and

$$\int_{\Gamma_3} g_3\, w_i\, d\Gamma = \sum_{k=1}^{n_{e^{\Gamma_3}}} \int_{\Gamma_3^{e_k}} g_3\, w_i\, d\Gamma, \tag{4.33}$$

where $n_{e^{\Gamma_2}}, n_{e^{\Gamma_3}}$ correspond to the number of boundary of the mesh elements on Γ_2 and Γ_3, respectively. Likewise, $\Gamma_2^{e_k}$ and $\Gamma_2^{e_k}$ denote the restriction of mesh element e_k to the boundaries Γ_2 and Γ_3.

5. RESULTS

This chapter embraces our theoretical knowledge and the computational results in the light of biological interpretation. We introduce with dimensional analysis which is a beneficial tool to understand the significance of units. After that the values of parameters used in the model are given with explanation and if they are experimented or estimated before, we direct the attention of the reader to the references they are given. Consequently, whether successful or not, we present a brief explanation of the graphics obtained.

5.1. Data and Parameters

5.1.1. Dimension Analysis

Mathematical modeling can be divided into some steps. The first one is to relate a physical or biological phenomenon to the mathematics which can be achieved by suitable identification of parameters and variables. The second step is to associate these variables via physical principles. We have done these two steps in the previous Modeling Chapter (3), at first we have tried to understand the physiological process and then we have set up a system of equations. In the second step, we have hypothesized that there should be a linear relation between MMP concentration and hydraulic conductivity of the tissue. The third step is try to attempt to find an answer to *"How are these two variables are related?"*. Dimensional analysis helps us as a guide for the selection of experiments which might have a potential to pose significant information. Rayleigh's reference to this point is really interesting [41]:

> "I have often been impressed by the scanty attention paid even by original workers in physics to the great principle of similitude. It happens not infrequently that results in the form of 'laws' are put forward as novelties on the basis of elaborate experiments which might have been predicted *a priori* after a few minutes' consideration".

If we plunge into the Equation 3.12 that we hypothesized:

$$\left[\frac{L^3T}{M}\right] = \left[\frac{L^3T}{M}\right] + [\frac{\textbf{unknown}}{\textbf{dimension}}] \times \left[\frac{M}{L^3}\right], \tag{5.1}$$

we obtain:

$$[\frac{\textbf{unknown}}{\textbf{dimension}}] = \left[\frac{L^6T}{M^2}\right]. \tag{5.2}$$

The dimension of the unknown coefficient might not be too familiar that we can identify. However, notice that:

$$\left[\frac{L^6T}{M^2}\right] = \left[\frac{L^2T}{M}\right]^2 \times \left[\frac{L^2}{T}\right]. \tag{5.3}$$

One can look into the Table 5.1 and deduce that the hydraulic conductivity of the interstitium K might depend on the concentration of MMP in the tissue together with its diffusion rate D_M and the hydraulic conductivity of vessel wall L_p just comparing their dimensions. There might be no relation between the concentration of MMPs and the hydraulic conductivity of vessel wall, but it is worth to search the literature with this direction. This is however, beyond our scope in this thesis so we defer this as a future work.

In the simulation, we obtain some of the parameters from the various articles whereas we estimate the others that we could not find an article about them.

In the Table 5.3, baseline values of parameters L_p, P_0, $\sigma(\pi_c - \pi_i)$ and K_0 are taken from Jain *et al.* 2007, [20]. Accordingly, baseline values of $\frac{S}{V}$ can be found in Jain 1987, [42]; λ_{Fb}, $1-\sigma$ and λ_d are from Öztürk *et al.* 2013, [29]. From Leu *et al.* 2000, [43] and Wu *et al.* 2013, [44], we can obtain baseline value of λ_{Fl} in tumor and in

Table 5.1. Units and Dimensions of Parameters and Variables Used in the Model-1.

Parameters		
Parameters and variables corresponding to tumor and its vasculature	**Units**	**Dimensions**
ϕ_F	–	Dimensionless
$\mathbf{v}_F$	$[mm/s]$	$\left[\frac{L}{T}\right]$
Γ_{Fb}	$[1/s]$	$\left[\frac{1}{T}\right]$
Γ_{Fl}	$[1/s]$	$\left[\frac{1}{T}\right]$
λ_{Fb}	$[1/mmHg.s]$	$\left[\frac{LT}{M}\right]$
λ_{Fl}	$[1/mmHg.s]$	$\left[\frac{LT}{M}\right]$
P	$[mmHg]$	$\left[\frac{M}{LT^2}\right]$
P_0	$[mmHg]$	$\left[\frac{M}{LT^2}\right]$
π_c	$[mmHg]$	$\left[\frac{M}{LT^2}\right]$
π_i	$[mmHg]$	$\left[\frac{M}{LT^2}\right]$
L_p	$[cm/mmHg.s]$	$\left[\frac{L^2T}{M}\right]$
$\frac{S}{V}$	$[cm^2/cm^3]$	$\left[\frac{1}{L}\right]$
$\mathbf{q}_F$	$[mm/s]$	$\left[\frac{L}{T}\right]$
K	$[cm^2/mmHg.s]$	$\left[\frac{L^3T}{M}\right]$
K_0	$[cm^2/mmHg.s]$	$\left[\frac{L^3T}{M}\right]$
Parameters and variables corresponding to drug concentration	**Units**	**Dimensions**
c	$[1/mm^3]$	$\left[\frac{1}{L^3}\right]$
c_p	$[1/mm^3]$	$\left[\frac{1}{L^3}\right]$
D_c	$[cm^2/s]$	$\left[\frac{L^2}{T}\right]$
k_E	–	Dimensionless
σ	–	Dimensionless
λ_d	$[1/s]$	$\left[\frac{1}{T}\right]$
λ_r	$[1/s]$	$\left[\frac{1}{T}\right]$

Table 5.2. Units and Dimensions of Parameters and Variables Used in the Model-2.

Parameters and variables corresponding to MMP activation	**Units**	**Dimensions**
M	$[mg/ml]$	$\left[\frac{M}{L^3}\right]$
M_p	$[mg/ml]$	$\left[\frac{M}{L^3}\right]$
λ_{Mn}	$[1/s]$	$\left[\frac{1}{T}\right]$
λ_{Mr}	$[1/s]$	$\left[\frac{1}{T}\right]$
λ_{Md}	$[1/s]$	$\left[\frac{1}{T}\right]$
D_M	$[cm^2/s]$	$\left[\frac{L^2}{T}\right]$
n	$[g/cm^3]$	$\left[\frac{M}{L^3}\right]$
D_E	$[cm^4/(mmHg)^2 s^3]$	$\left[\frac{L^6 T}{M^2}\right]$

normal cells, respectively. Moreover, D_c, k_E, λ_r, M_p, n and $t_{1/2}$ can be accessed from Pluen *et al.* 2001, [45], Reddy *et al.* 2006, [46], Laginha *et al.* 2005, [47], Goodman *et al.* 2007, [48], Wen *et al.* 2012, [49] and Gabizon *et al.* 1994, [50], respectively. Finally, baseline values of λ_{Mn}, λ_{Mr} and λ_{Md} are obtained from Kim *et al.* 2009, [51], whereas baseline values of D_M and D_E are estimated in this work.

Table 5.3. Parameters Related to the Transport of 100 nm Liposomes.

Parameter	**Unit**	**Baseline Value**	
		Tumor	
L_p	$[cm/mmHg.s]$	1.86×10^{-6}[a]	3.6×10^{-8}
$\frac{S}{V}$	$[cm^2/cm^3]$	200	70
λ_{Fb}	$[1/mmHg.s]$	3.72×10^{-4}	2.56×10^{-6}
λ_{Fl}	$[1/mmHg.s]$	0	6.66×10^{-4}[e]
P_0	$[mmHg]$	15	15
$\sigma(\pi_c - \pi_i)$	$[mmHg]$	2.2×10^{-4}	9.1
K_0	$[cm^2/mmHg.s]$	2.5×10^{-7}	2.5×10^{-7}
D_c	$[cm^2/s]$	2.5×10^{-9}	2.5×10^{-9}
k_E	–	0.35	0.35
$1 - \sigma$	–	0.87	0
λ_d	$[1/s]$	4×10^{-6}	1.4×10^{-7}
λ_r	$[1/hours]$	1/135	1/135
M_p	$[mg/ml]$	0.1	0.1
λ_{Mn}	$[1/s]$	6.94×10^{-8}	-
λ_{Mr}	$[1/s]$	5×10^{-5}	-
λ_{Md}	$[1/s]$	1×10^{-6}	1×10^{-6}
D_M	$[cm^2/s]$	1.86×10^{-6}	1.86×10^{-6}[k]
n	$[g/cm^3]$	1	-
D_E	$[cm^4/(mmHg)^2 s^3]$	1	-
$t_{1/2}$	hours	45.2	45.2

5.2. Graphics and Interpretation

We try to simulate the effect of MMP injection into the tumor tissue to the IFP and drug concentration in the tissue. In order to do this, we try to solve the equations with constant hydraulic conductivity K_0 (see 5.3) and changing K with MMP. In a previous work, Professor Unlu and the modeling group [29] attempted to observe the effect of vascularization to the IFP, drug concentration and drug distribution. Since the hydraulic conductivity and its impact to vascularization have not known well yet [4], they introduced a 50% percent change in the tumor vessel surface density ($\frac{S}{V}$), 80% percent decrease in tumor vessel hydraulic conductivity (L_p) and 60% percent decrease in tumor vascular network permeability for the vascular normalization therapy. In this study, we do not hold these vascular normalization assumptions to see the real effect of increasing hydraulic conductivity. However, we observe that this assumption tightly depends on the radius of tumor. We hereby investigate the results by grouping them according to the tumor radius. The first four plots (Figures 5.1, 5.3 and Figures 5.2, 5.4) belong to the tumors with radius $1 \leq R_0 \leq 2$, respectively. Solid blue lines refer to the tumors with constant hydraulic conductivity K whereas the green lines refer to the ones with changing hydraulic conductivity via MMP activation.

It can be seen that in (figures 5.1 and 5.2), there is a significant reduction of IFP (33% and 20% decreases) in the tumor center. Accordingly, inside the tumors, the IFP is uniformly elevated and decreases drastically to normal values which causes a steep pressure gradient. As a result, interstitial fluid escapes from the tumor periphery into the healthy tissue, which might results in metastasis. On the other hand, for small radii tumors, our model supports the normalization therapy: The reduction of IFP restores pressure gradients across the vessel wall and helps to a deeper penetration of molecules into tumor [32]. However, drug concentration of small radii tumors is different even for $R_0 = 1\ mm$ and $R_0 = 2\ mm$. The drug injected to the tumor for $R_0 = 1\ mm$ is distributed nearly same in the untreated tumor case (Figure 5.3 green and blue lines, respectively) whereas the uniformity of drug distribution is more preserved in treated tumor with MMP activation (Figure 5.4 green and blue lines, respectively).

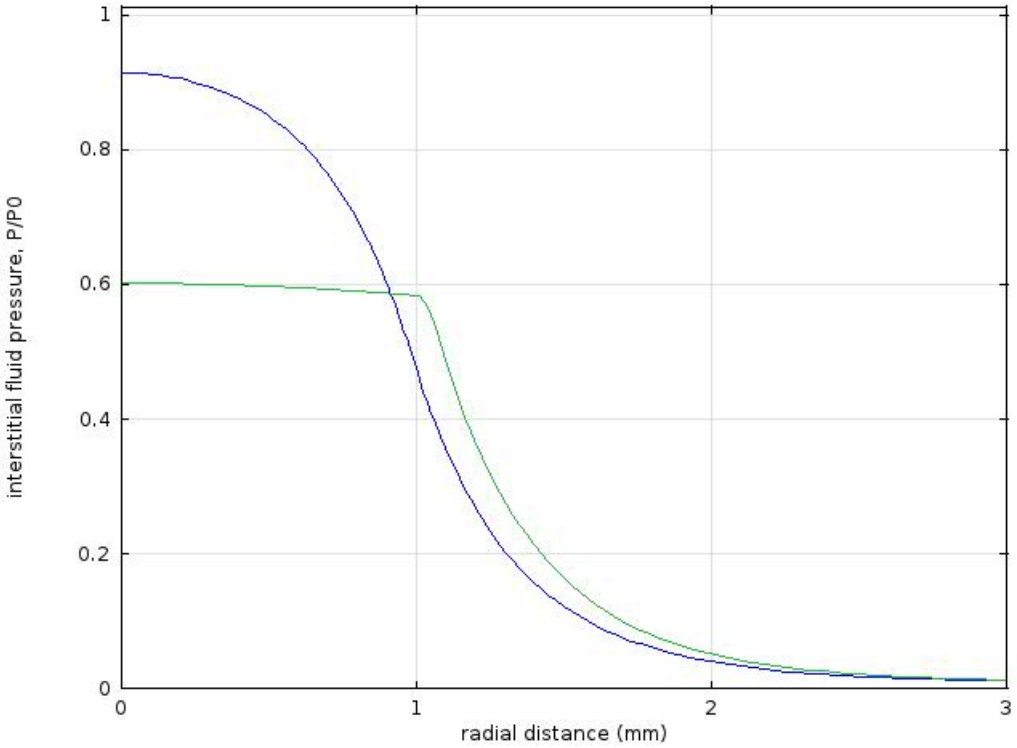

Figure 5.1. IFP when Tumor Radius Achieves $R_0 = 1\ mm$.

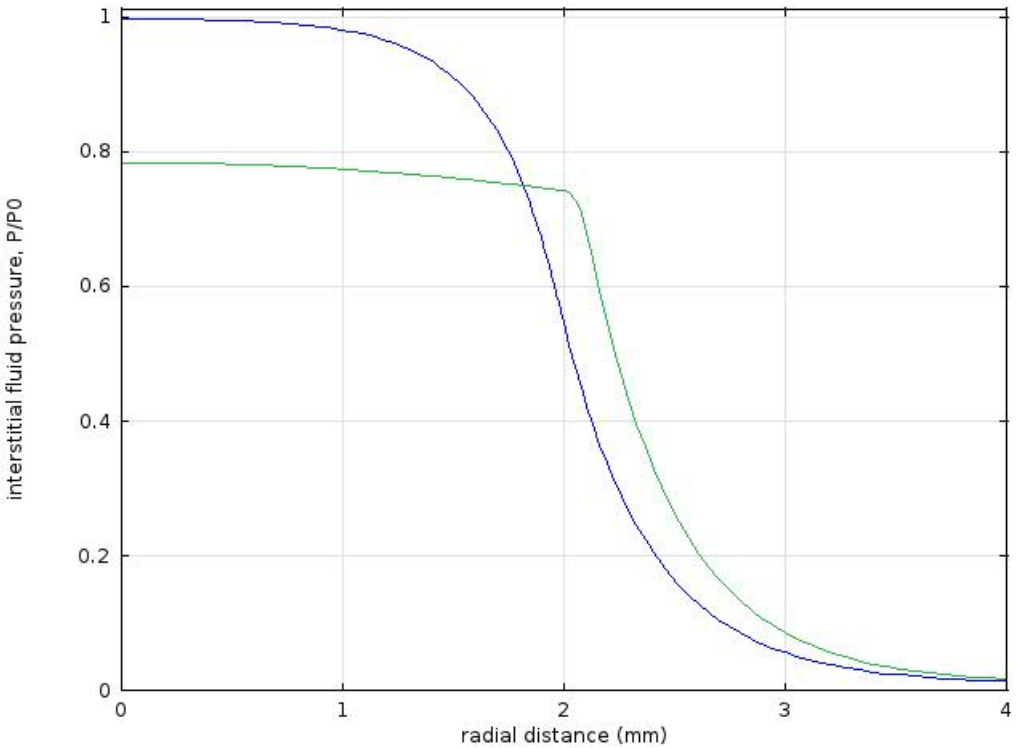

Figure 5.2. IFP when Tumor Radius Achieves $R_0 = 2\ mm$.

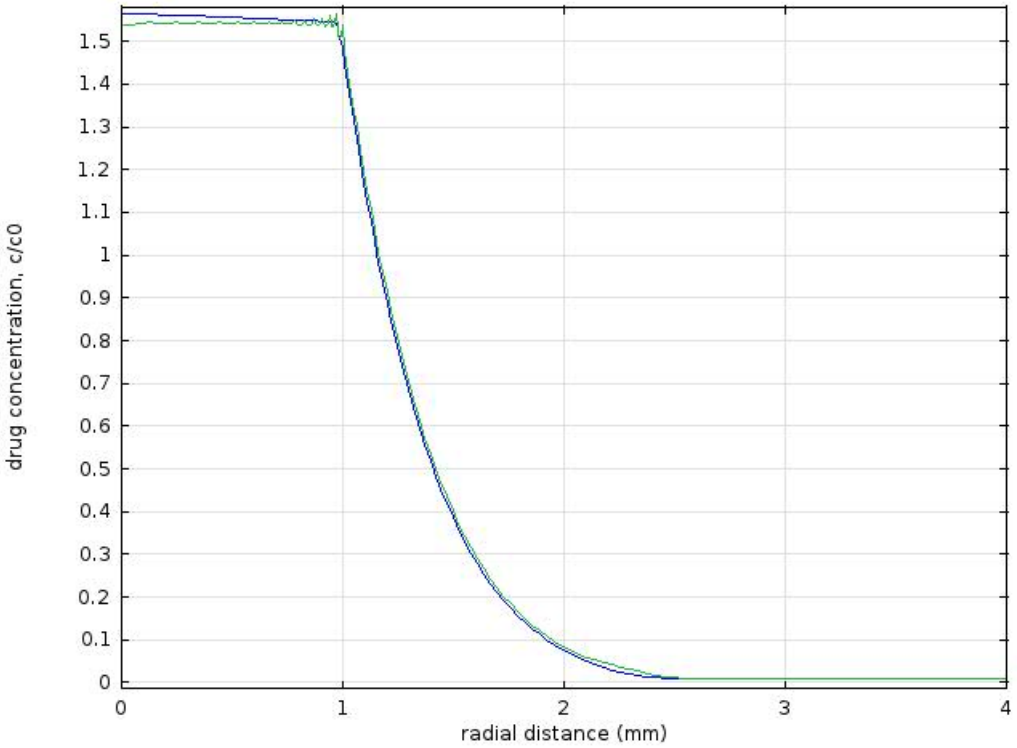

Figure 5.3. Drug Concentration for $R_0 = 1\ mm$.

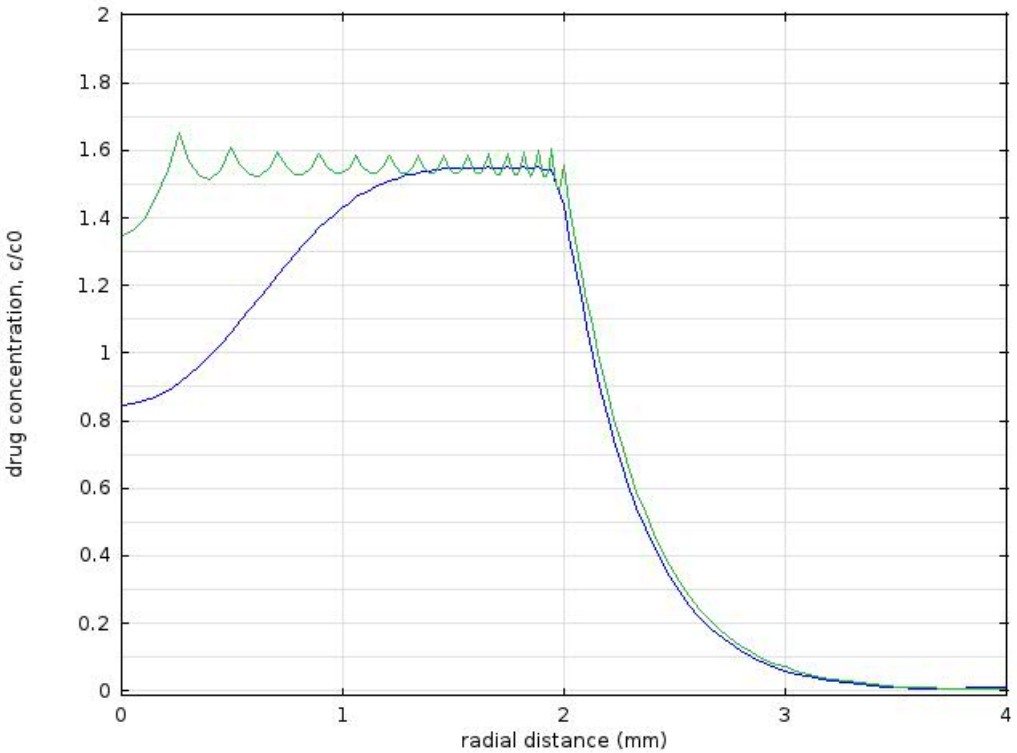

Figure 5.4. Drug Concentration for $R_0 = 2\ mm$.

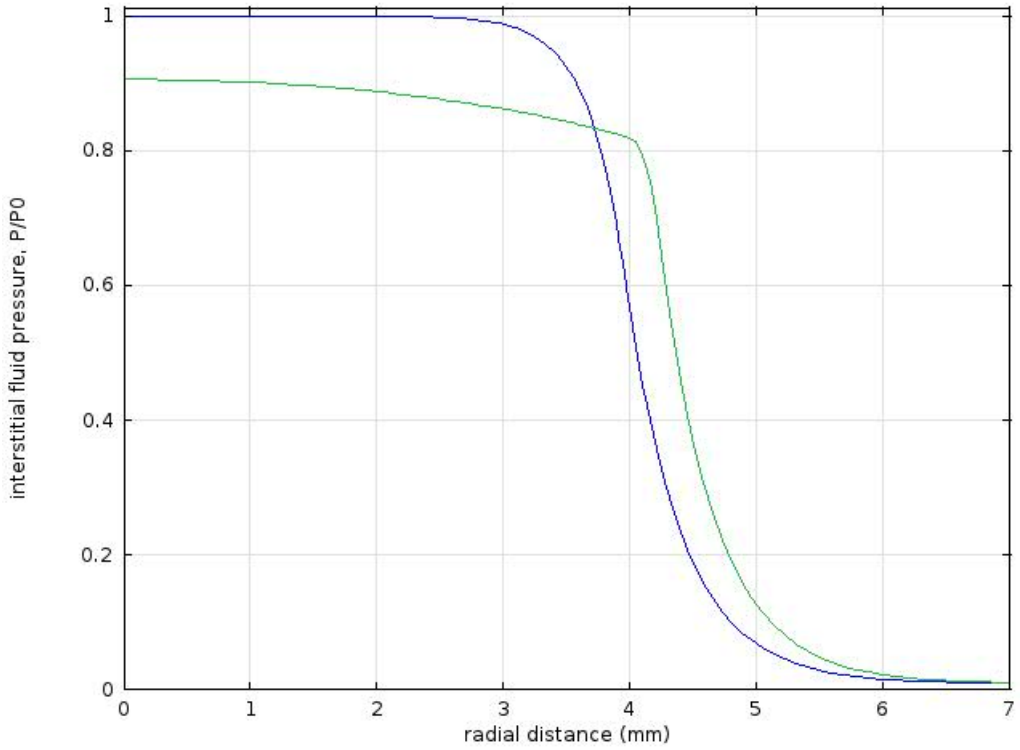

Figure 5.5. IFP when Tumor Radius Achieves $R_0 = 4\ mm$.

For medium size tumors $4 \leq R_0 \leq 6\ mm$, the IFP is still lower than untreated tumors (Figures 5.5 and 5.6) but now this reduction is lower comparing to the small size tumors. Moreover, around the boundary the IFP drops slowly in the treated tumor which is crucial in therapies. However, the drug concentration in medium size tumors in our model might not be very realistic since it oscillates and the oscillation increases around the tumor center. When tumor size increases in the center hypoxia occurs which might cause apoptosis, so it may be deduced the exposure of the drug is still better but getting closer to the tumor center might lead drastic drops (see Figures 5.7 and 5.8).

When the tumor size is large enough $8 \leq R_0 \leq 15\ mm$, the treatment with MMPs is not beneficial as in the small radii tumors regarding the IFP. Increasing hydraulic conductivity with MMPs still prevent steep drops in IFP around the boundary but for efficacy, the more is required (see Figures 5.9 and 5.10). IFP should be decreased and this might be possible for other normalization processes. The drug concentration has

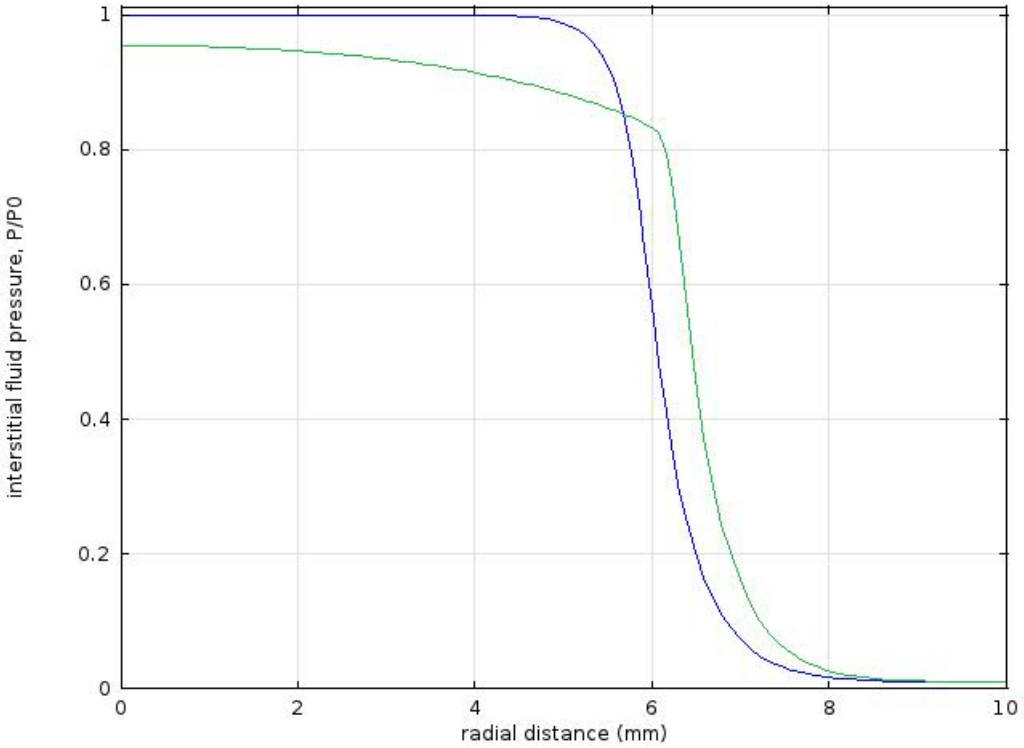

Figure 5.6. IFP when Tumor Radius Achieves $R_0 = 6\ mm$.

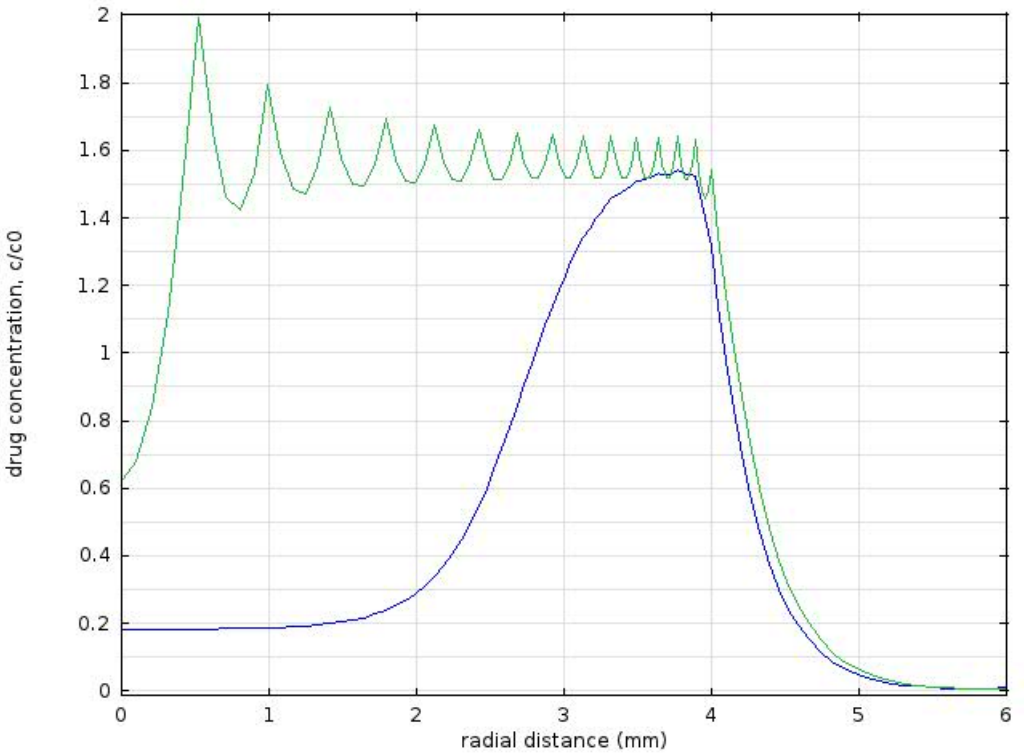

Figure 5.7. Drug Concentration for $R_0 = 4\ mm$.

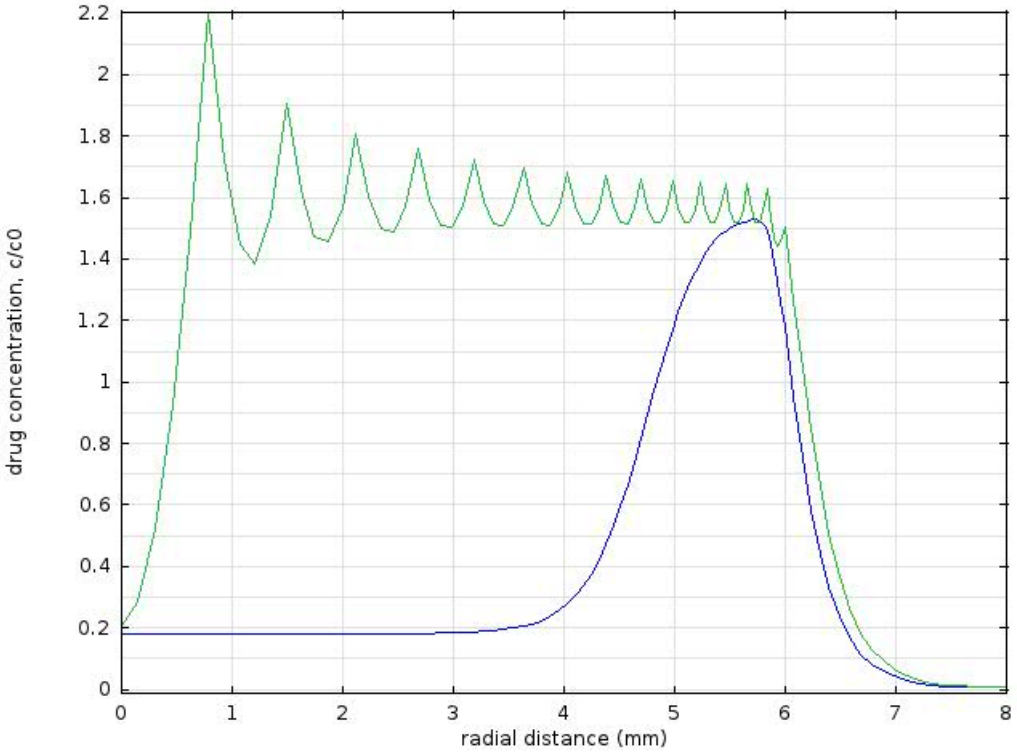

Figure 5.8. Drug Concentration for $R_0 = 6\ mm$.

large oscillations in our treated case (Figure 5.11), however for (Figure 5.12) the drug concentration is uniformly distributed and the behaviour of the drug demonstrates the success of the MMP effect.

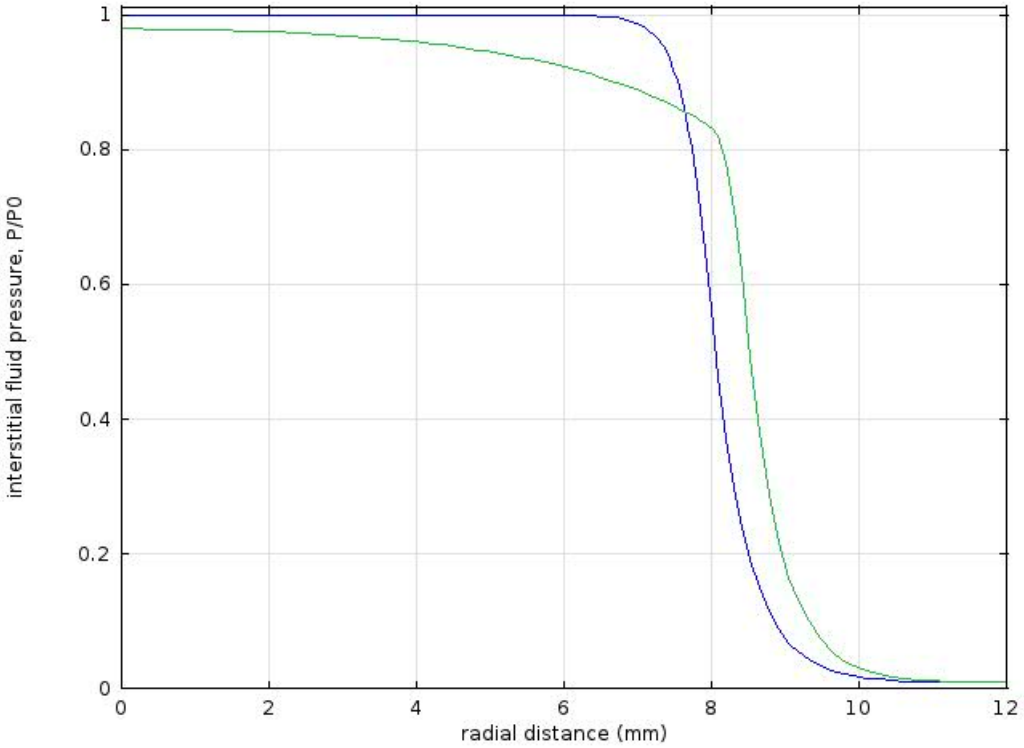

Figure 5.9. IFP when Tumor Radius Achieves $R_0 = 8\ mm$.

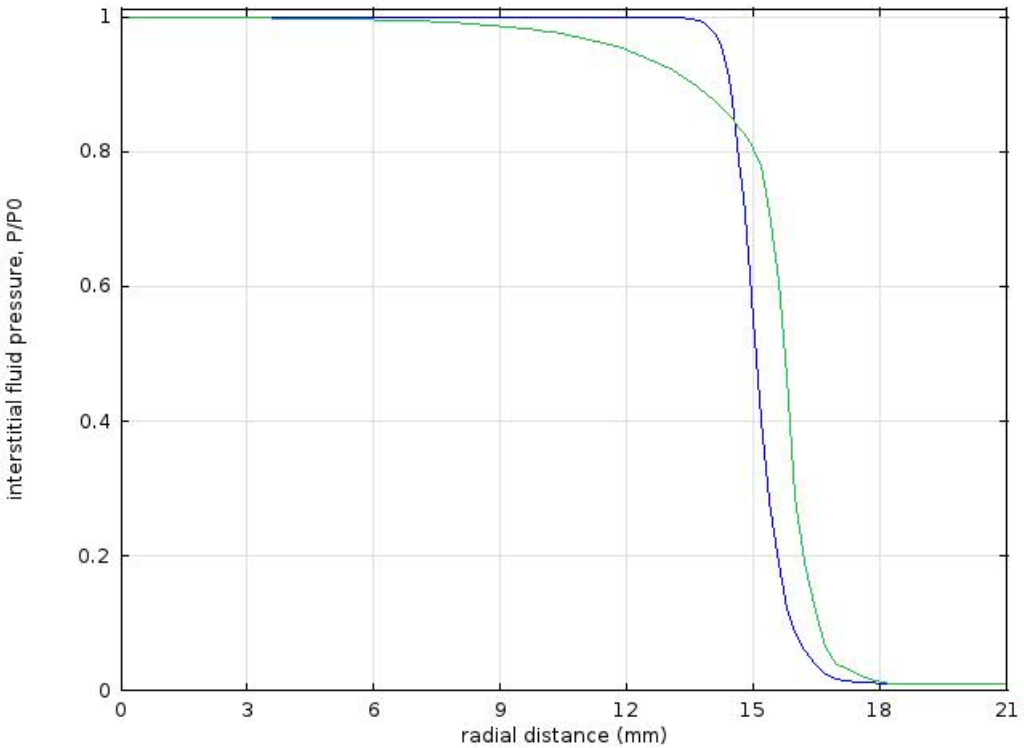

Figure 5.10. IFP when Tumor Radius Achieves $R_0 = 15\ mm$.

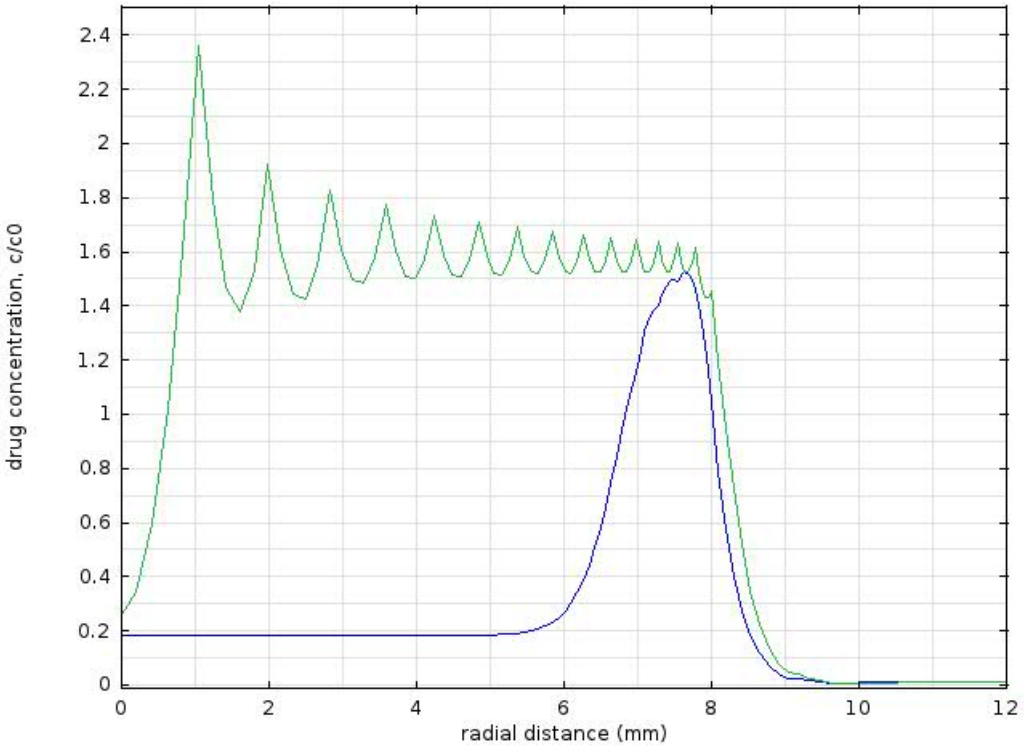

Figure 5.11. Drug Concentration for $R_0 = 8\ mm$.

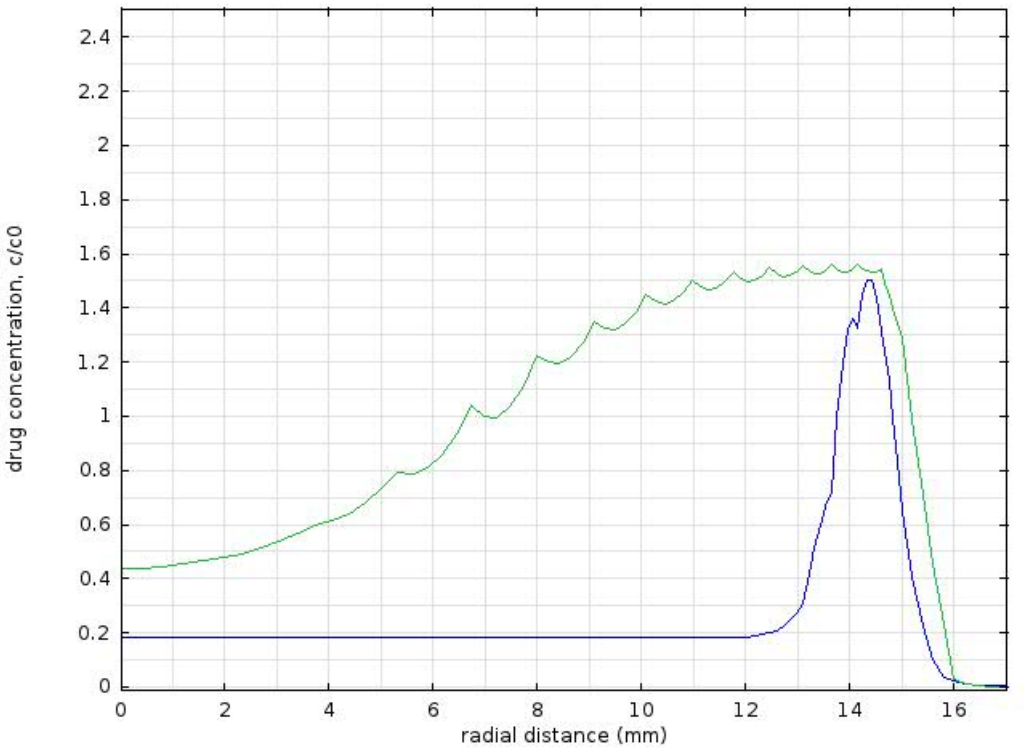

Figure 5.12. Drug Concentration for $R_0 = 15\ mm$.

6. DISCUSSION AND FUTURE WORK

In this thesis, we experienced that a mathematical model and its simulation has tremendous advantages comparing to the real laboratory experiments. First of all, the parameters and their estimations have no restrictions except time and computational costs. The uniqueness of a live body (whether human or animal) does not give enough freedom to a doctor for chemotherapy, each treatment should be specific to the patient. However the current developments do not suffice to be handled with each patients. Rather, the necessary therapeutic agents are mixed with some proportions and this depends strictly on the doctors' before experiences and their knowledges. Naturally, cancer still poses its severity on the mortality degree over the world. That's why in U.S and other some countries the medicine faculties have interdisciplinary departments, they need physicists for imaging; applied mathematicians for successful and valid models; chemists and engineers for better drug designs. Specialization in each discipline with a unique motivation will be the milestone for developments.

We used COMSOL Multiphysics program during the simulations, it might be a future aim to work on other simulation processes. For instance, Soltani and Chen [52] developed a numerical model for fluid flow assuming not only spherical tumors, they also investigated non-spherical tumors like the prolate and oblate tumors with an element-based finite volume method (EB-FVM) and the Semi Implicit Method for Pressure Linked Equations (SIMPLE) algorithm. So a better analysis and best suitable choice of the parameters will be our future work. Furthermore, the last article of Lowengrub and his research group [44] made us believed that we are on the right way.

We only studied for the liposomes with 100 nm based on the positive results of the articles [29] and [6]. For this reason, some questions such as *Is there any relation between MMP concentration and hydraulic conductivity of vessel wall?*, *What is the effect of MMPs on different type drugs? (Nanoparticles, oncolytic viruses (HSV), lipoplex)* are still waiting to be answered and this thesis gave a concrete motivation to

plunge into the drug delivery modeling. We might use other therapeutic drugs in our improved model by taking the articles [30], [16], [31] and [48] as a basis.

On the other side, the beneficial side of MMPs might be restricted comparing to its side effect to other cells. One should aware of the fact that the drugs developed as MMP anti-targets might cause other unexpected diseases in human body since the properties of MMPs are not completely known. Mathematical modeling and computational approach might become parts of the developments at this step with optimizing the beneficial sides of MMPs for drug delivery and the biologists hereby might find more opportunities to investigate and explore unknown sides of these MMPs.

APPENDIX A: FUNCTIONAL ANALYSIS FACTS

We prefer concerning some necessary information about functional analysis in this appendix section since we did not want to interrupt the flow of the "Simulation" Chapter. The necessary definitions and theorems in Kress' book [39] are covered here.

Definition A.1. *Let X be a complex vector space. Then, a function*

$$S : X \times X \to \mathbb{C} \tag{A.1}$$

is called sesquilinear if it is linear in the first variable and conjugate linear in the second variable, which is:

$$S(\alpha u + \beta v, w) = \alpha S(u, w) + \beta S(v, w) \tag{A.2}$$

and

$$S(u, \alpha v + \beta w) = \overline{\alpha} S(u, v) + \overline{\beta} S(u, w) \tag{A.3}$$

for all $u, v, w \in X$ and for all $\alpha, \beta \in \mathbb{C}$. In fact, if X is a real vector space, then S is called bilinear.

Definition A.2. *A sesquilinear function S on a normed space X is called bounded if*

$$|S(u, v)| \leq C||u||||v|| \tag{A.4}$$

for all $u, v \in X$ and for some positive constant C.

Definition A.3. *A sesquilinear function S on a normed space X is called strictly coercive provided that*

$$Re(S(u, v)) \geq c||u||^2 \tag{A.5}$$

for all $u \in X$ and for some positive constant c.

Definition A.4. *A linear operator $A : X \to X$ in a pre-Hilbert space X is called strictly coercive provided that*

$$Re(\langle Au, u\rangle) \geq c||u||^2 \tag{A.6}$$

for all $u \in X$ and for some positive constant c.

Theorem A.1. *(Riesz's Theorem) Let X be a Hilbert Space, then for each bounded linear functional $F : X \to \mathbb{C}$, there exists a unique element $f \in X$ such that*

$$F(u) = \langle u, f\rangle \tag{A.7}$$

for all $u \in X$.

The following theorem states a unique solution to Galerkin's Method:

Theorem A.2 (Céa's Lemma)**.** *(Céa's Lemma) Let $A : X \to X$ be a bounded strictly coercive linear operator on a Hilbert Space X, then Galerkin Equations (4.2) have a unique solution $u_n \in X_n$. Moreover,*

$$||u_n - u|| \leq M \inf_{v \in X_n} ||v - u||, \tag{A.8}$$

where M is some constant depending on the operator A.

Theorem A.3. *(Lax-Milgram Theorem) In a Hilbert Space X, a bounded and strictly coercive linear operator $A : X \to X$ with coercivity constant $c > 0$ has a bounded inverse $A^{-1} : X \to X$ with $||A^{-1}|| \leq 1/c$.*

Theorem A.4. *(Lax-Milgram Lemma) Let S be a bounded, strictly coercive sesquilinear function and $F : X \to \mathbb{C}$ (or $\mathbb{R}$) a bounded linear functional on a Hilbert Space X. Then there exists a unique $u \in X$ so that*

$$S(v, u) = F(v) \tag{A.9}$$

for all $v \in X$.

Definition A.5. *A function* $u \in L^2[a,b]$ *is said to have a weak derivative* $u' \in L^2[a,b]$ *if*

$$\int_a^b u\, v'\, dx = -\int_a^b u'\, v\, dx \tag{A.10}$$

for all $v \in C^1[a,b]$ *with* $v(a) = v(b) = 0$.

Theorem A.6. *(Sobolev Spaces) The linear space*

$$H^1[a,b] = \{u \in L^2[a,b] : u' \in L^2[a,b]\} \tag{A.11}$$

is a Hilbert space named Sobolev space with this inner product:

$$\langle u, v\rangle_{H^1} := \int_a^b (uv + u'v')dx. \tag{A.12}$$

Notice that the space

$$H_0^1[a,b] = \{u \in H^1[a,b] : u(a) = u(b) = 0\} \tag{A.13}$$

is a complete subspace of $H^1[a,b]$.

REFERENCES

1. Byrne, H. M., "Dissecting Cancer Through Mathematics: From the Cell to the Animal Model", *Nature Reviews. Cancer*, Vol. 10, No. 3, pp. 221–230, 2010.

2. Martins, M., S. Ferreirajr and M. Vilela, "Multiscale Models for the Growth of Avascular Tumors", *Physics of Life Reviews*, Vol. 4, No. 2, pp. 128–156, 2007.

3. Cristini, V. and J. Lowengrub, *Multiscale Modeling of Cancer: An Integrated Experimental and Mathematical Modeling Approach*, Cambridge University Press, Cambridge, 2010.

4. Fukumura, D. and R. Jain, "Tumor Microvasculature and Microenvironment: Targets for Anti-angiogenesis and Normalization", *Microvascular Research*, Vol. 74, No. 2-3, pp. 72–84, 2007.

5. Gialeli, C., A. D. Theocharis and N. K. Karamanos, "Roles of Matrix Metalloproteinases in Cancer Progression and Their Pharmacological Targeting.", *The FEBS Journal*, Vol. 278, No. 1, pp. 16–27, 2011.

6. Zheng, X., B. Goins, I. Cameron, C. Santoyo, A. Bao, V. Frohlich and G. Fullerton, "Ultrasound-Guided Intratumoral Administration of Collagenase-2 Improved Liposome Drug Accumulation in Solid Tumor Xenografts.", *Cancer Chemotherapy and Pharmacology*, 2010.

7. Milosevic, M., S. J. Lunt, E. Leung, J. Skliarenko, P. Shaw, A. Fyles and R. P. Hill, "Interstitial Permeability and Elasticity in Human Cervix Cancer.", *Microvascular Research*, Vol. 75, No. 3, pp. 381–90, 2008.

8. Bellomo, N., E. Angelis and L. Preziosi, "Review Article: Multiscale Modeling and Mathematical Problems Related to Tumor Evolution and Medical Therapy", *Journal of Theoretical Medicine*, Vol. 5, No. 2, pp. 111–136, 2003.

9. Hartwell, L. H., J. J. Hopfield, S. Leibler and A. W. Murray, "From Molecular to Modular Cell Biology", *Nature*, Vol. 402, No. 6761 Suppl, pp. C47–C52, 1999.

10. Gatenby, R. A. and P. K. Maini, "Mathematical Oncology: Cancer Summed Up", *Nature*, Vol. 421, No. 6921, p. 321, 2003.

11. Friedman, A., "What is Mathematical Biology and How Useful is it?", *Notices of the AMS*, Vol. 57, No. 7, pp. 851–860, 2010.

12. Deisboeck, T. S., Z. Wang, P. Macklin and V. Cristini, "Multiscale Cancer Modeling", *Annual Review of Biomedical Engineering*, Vol. 13, pp. 127–155, 2011.

13. Preziosi, L., *Cancer Modelling and Simulation*, Chapman & Hall/CRC Mathematical & Computational Biology, Taylor & Francis, Boca Raton, FL, 2003.

14. Rejniak, K. A. and L. J. McCawley, "Current Trends in Mathematical Modeling of Tumor-Microenvironment Interactions: A Survey of Tools and Applications.", *Experimental Biology and Medicine (Maywood, N.J.)*, Vol. 235, No. 4, pp. 411–423, 2010.

15. Macklin, P. and J. Lowengrub, "Nonlinear Simulation of the Effect of Microenvironment on Tumor Growth.", *Journal of Theoretical Biology*, Vol. 245, No. 4, pp. 677–704, 2007.

16. Mok, W., *Improving the Delivery and Efficacy of a Cancer Therapeutic Via Extracellular Matrix Modification*, Ph.D. Thesis, Massachusetts Institute of Technology, Department of Chemical Engineering, 2008.

17. Egeblad, M., "Live Imaging Shows Response to Cancer Drugs can be Boosted by Altering Tumor Microenvironment", *Cold Spring Harbor Laboratory*, 2012.

18. Kim, Y., M. A. Stolarska and H. G. Othmer, "The Role of the Microenvironment in Tumor Growth and Invasion", *Progress in Biophysics and Molecular Biology*,

Vol. 106, No. 2, pp. 353–379, 2011.

19. Wirtz, D., K. Konstantopoulos and P. C. Searson, "The Physics of Cancer: The Role of Physical Interactions and Mechanical Forces in Metastasis.", *Nature Reviews. Cancer*, Vol. 11, No. 7, pp. 512–22, 2011.

20. Jain, R. K., R. T. Tong and L. L. Munn, "Effect of Vascular Normalization by Antiangiogenic Therapy on Interstitial Hypertension, Peritumor Edema, and Lymphatic Metastasis: Insights from a Mathematical Model.", *Cancer Research*, Vol. 67, No. 6, pp. 2729–2735, 2007.

21. Sounni, N., A. Paye, L. Host and A. Noël, "MT-MMPS as Regulators of Vessel Stability Associated with Angiogenesis.", *Frontiers in Pharmacology*, Vol. 2, 2011.

22. Löffek, S., O. Schilling and C.-W. W. Franzke, "Biological Role of Matrix Metalloproteinases: A Critical Balance.", *The European Respiratory Journal*, 2010.

23. Remacle, A. G., V. S. Golubkov, S. A. Shiryaev, R. Dahl, J. L. Stebbins, A. V. Chernov, A. V. Cheltsov, M. Pellecchia and A. Y. Strongin, "Novel MT1-MMP Small-Molecule Inhibitors Based on Insights into Hemopexin Domain Function in Tumor Growth.", *Cancer Research*, Vol. 72, No. 9, pp. 2339–49, 2012.

24. Egeblad, M. and Z. Werb, "New Functions for the Matrix Metalloproteinases in Cancer Progression.", *Nature Reviews. Cancer*, Vol. 2, No. 3, pp. 161–74, 2002.

25. López-Otín, C., L. Palavalli and Y. Samuels, "Protective Roles of Matrix Metalloproteinases: From Mouse Models to Human Cancer.", *Cell Cycle*, Vol. 8, No. 22, 2009.

26. Tremblay, P., M. Beaudet, E. Tremblay, N. Rueda, T. Thomas and L. Vallières, "Matrix Metalloproteinase 2 Attenuates Brain Tumour Growth, While Promoting Macrophage Recruitment and Vascular Repair.", *The Journal of Pathology*, Vol. 224, No. 2, pp. 222–33, 2011.

27. Zucker, S. and J. Cao, "Selective Matrix Metalloproteinase (MMP) Inhibitors in Cancer Therapy: Ready for Prime Time?", *Cancer Biology & Therapy*, Vol. 8, No. 24, pp. 2371–3, 2009.

28. Dufour, A. and C. M. Overall, "Missing the Target: Matrix Metalloproteinase Antitargets in Inflammation and Cancer.", *Trends in Pharmacological Science*, 2013.

29. Ozturk, D., S. Yonucu and M. B. Unlu, *Influence of Vascular Normalization on Interstitial Flow and Nanoparticle Delivery in Tumors*, 2013, Preprint submitted to Journal of Theoretical Biology.

30. Mok, W., Y. Boucher and R. Jain, "Matrix Metalloproteinases-1 and -8 Improve the Distribution and Efficacy of an Oncolytic Virus.", *Cancer Research*, Vol. 67, No. 22, pp. 10664–8, 2007.

31. Kato, M., Y. Hattori, M. Kubo and Y. Maitani, "Collagenase-1 Injection Improved Tumor Distribution and Gene Expression of Cationic Lipoplex.", *International Journal of Pharmacology*, Vol. 423, No. 2, pp. 428–34, 2012.

32. Jain, R. K. and T. Stylianopoulos, "Delivering Nanomedicine to Solid Tumors.", *Nature reviews. Clinical oncology*, Vol. 7, No. 11, pp. 653–664, 2010.

33. Amar, M., A. Goriely, M. Müller and L. Cugliandolo, *New Trends in the Physics and Mechanics of Biological Systems: Lecture Notes of the Les Houches Summer School: Volume 92, July 2009*, Ecole de Physique Des Houches, OUP Oxford, New York, 2011.

34. Higgins, B. G., *Balance Equations and Conservation of Mass*, 2004, `http://www.ekayasolutions.com/ECH256win_08.php`, accessed at May 2013.

35. Truskey, G., F. Yuan and D. Katz, *Transport Phenomena in Biological Systems*, Pearson Prentice Hall Bioengineering, Pearson Education, Upper Saddle River,

New Jersey, 2009.

36. Xu, M. and L. V. Wang, "Photoacoustic Imaging in Biomedicine", *Review of Scientific Instruments*, Vol. 77, No. 4, pp. 041101+, 2006.

37. Ren, K., "Recent Developments in Numerical Techniques for Transport-Based Medical Imaging Methods", *Communications in Computational Physics*, Vol. 8, No. 1, pp. 1–50, 2010.

38. Bangerth, W. and A. Joshi, "Adaptive Finite Element Methods for the Solution of Inverse Problems in Optical Tomography", *Inverse Problems*, Vol. 24, No. 3, p. 034011, 2008.

39. Kress, R., *Numerical Analysis*, Graduate Texts in Mathematics, Springer-Verlag, New York, 1998.

40. Segal, I. A., *Finite Element Methods For The Incompressible Navier-Stokes Equations*, 2012, `ta.twi.tudelft.nl/users/vuik/burgers/fem_notes.pdf`, accessed at May 2013.

41. Huntley, H., *Dimensional Analysis*, Dover Books. S, Dover Publications, New York, 1967.

42. Jain, R. K., "Transport of Molecules Across Tumor Vasculature", *Cancer and Metastasis Reviews*, Vol. 6, No. 4, pp. 559–593, 1987.

43. Leu, A., D. Berk, A. Lymboussaki, K. Alitalo and R. Jain, "Absence of Functional Lymphatics within a Murine Sarcoma: A Molecular and Functional Evaluation.", *Cancer Research*, Vol. 60, No. 16, pp. 4324–7, 2000.

44. Wu, M., H. B. Frieboes, S. R. McDougall, M. A. J. Chaplain, V. Cristini and J. Lowengrub, "The Effect of Interstitial Pressure on Tumor Growth: Coupling with the Blood and Lymphatic Vascular Systems.", *Journal of Theoretical Biology*,

Vol. 320, pp. 131–151, 2013.

45. Pluen, A., Y. Boucher, S. Ramanujan, T. McKee, T. Gohongi, E. di Tomaso, E. Brown, Y. Izumi, R. Campbell, D. Berk and R. Jain, "Role of Tumor-Host Interactions in Interstitial Diffusion of Macromolecules: Cranial vs. Subcutaneous Tumors.", *Proceedings of National Academy of Sciences of the United States of America*, Vol. 98, No. 8, pp. 4628–33, 2001.

46. Reddy, S., D. Berk, R. Jain and M. Swartz, "A Sensitive in vivo Model for Quantifying Interstitial Convective Transport of Injected Macromolecules and Nanoparticles.", *Journal of Applied Physiology*, 2006.

47. Laginha, K., S. Verwoert, G. Charrois and T. Allen, "Determination of Doxorubicin Levels in Whole Tumor and Tumor Nuclei in Murine Breast Cancer Tumors.", *Clinical Cancer Research*, Vol. 11, No. 19 Pt 1, pp. 6944–9, 2005.

48. Goodman, T., P. Olive and S. Pun, "Increased Nanoparticle Penetration in Collagenase-Treated Multicellular Spheroids.", *International Journal of Nanomedicine*, Vol. 2, No. 2, pp. 265–74, 2007.

49. Wen, F., R. Thisted, D. Rowley and H. Schreiber, "A Systematic Analysis of Experimental Immunotherapies on Tumors Differing in Size and Duration of Growth.", *Oncoimmunology*, Vol. 1, No. 2, pp. 172–178, 2012.

50. Gabizon, A., R. Catane, B. Uziely, B. Kaufman, T. Safra, R. Cohen, F. Martin, A. Huang and Y. Barenholz, "Prolonged Circulation Time and Enhanced Accumulation in Malignant Exudates of Doxorubicin Encapsulated in Polyethylene-Glycol Coated Liposomes.", *Cancer Research*, Vol. 54, No. 4, pp. 987–92, 1994.

51. Kim, Y., S. Lawler, M. O. Nowicki, E. A. Chiocca and A. Friedman, "A Mathematical Model for Pattern Formation of Glioma Cells Outside the Tumor Spheroid core", *Journal of Theoretical Biology*, Vol. 260, No. 3, pp. 359 – 371, 2009.

52. Soltani, M. and P. Chen, "Effect of Tumor Shape and Size on Drug Delivery to Solid Tumors.", *Journal of Biological Engineering*, Vol. 6, No. 1, p. 4, 2012.

53. Yonucu, S., *Mathematical Modeling of MMPS in Cancer*, Master's Thesis, Boğaziçi University, Graduate Program in Physics, 2012.

54. Rowe, R. and S. Weiss, "Breaching the Basement Membrane: Who, When and How?", *Trends in Cell Biology*, Vol. 18, No. 11, pp. 560–74, 2008.